

Supporting Material for

Reversible Luminescent Reaction of Amines with Copper(I) Cyanide.

Amanda N. Ley,^a Lars E. Dunaway,^a Timothy P. Brewster,^a

Matthew D. Dembo,^a T. David Harris,^b François Baril-Robert,^c

Xiaobo Li,^c Howard H. Patterson^c and Robert D. Pike*^a

^a Department of Chemistry, College of William and Mary,
Williamsburg, VA 23187-8795.

Fax: (757)221-2715; Tel: (757)221-2555; E-mail: rdpike@wm.edu

^b Department of Chemistry, University of California,
Berkeley, CA 94720-1460

^c Department of Chemistry, University of Maine,
Orono, ME 04469-5706

Contents

Experimental Details.....	3
Luminescence Photograph of Authentic (CuCN)L _n Compounds.....	9
X-ray Crystal Structure Tables	
Table S1. Crystal data and structure refinement for 2b	10
Table S2. Crystal data and structure refinement for 6a	11
Table S3. Crystal data and structure refinement for 8	12
Table S4. Crystal data and structure refinement for 9	13
Table S5. Crystal data and structure refinement for 12	14
Table S6. Crystal data and structure refinement for 13	15
Table S7. Selected bond lengths and angles for all complexes.....	16
Thermogravimetric Traces.....	19
Experimental and Calculated X-ray Powder Patterns for (CuCN)L _n	28
X-ray Powder Patterns for CuCN + L.....	46
Luminescence Spectra.....	57

Experimental

Materials and Methods. All reagents were purchased from Aldrich or Acros and used without purification. Analyses for C, H, and N were carried out by Atlantic Microlabs, Norcross, GA. Steady-state photoluminescence at ambient and reduced temperature were collected using a Photon Technology International Model Quanta-Master-1046 spectrophotometer equipped with a 75 W xenon lamp. Wavelengths were selected with two excitation monochromators and a single emission monochromator. A Model LT-3-110-Heli-Trans cryogenic liquid transfer system equipped with a temperature controller was used to record luminescence spectra as a function of temperature. IR measurements were made on KBr pellets using a Digilab FTS 7000 FTIR spectrophotometer. Thermogravimetric analyses (TGA) were conducted using a TA Instruments Q500 in the dynamic (variable temp.) mode with a maximum heating rate of 50 °C/min. to 300 °C under 60 mL/min. N₂ flow.

Syntheses

(CuCN)(Py)₂, 1a. Copper(I) cyanide (0.150 g, 1.67 mmol) was suspended in about 5 mL Py in a sealed tube under Ar. The mixture was heated to 70 °C in an oil bath overnight without stirring. After cooling, the suspended solid was collected by means of filtration, washed with diethyl ether, and then air dried for 15 min. A yellow powder was isolated (0.393 g, 1.59 mmol, 94.7%). IR (KBr pellet, cm⁻¹) 2124.4, 2103.8, 2086.1. Anal. Calcd for C₁₁H₁₀N₃Cu: C, 53.32; H, 4.07; N, 16.96. Found: C, 52.31; H, 3.96; N, 16.71. TGA Calcd for (CuCN)(Py) 68.0. Found: 70.5 (35–55 °C). Calcd for (CuCN)₃(Py)₂: 57.4 Found: 56.1 (55–85 °C). Calcd for (CuCN)₃(Py): 46.8. Found: 48.5 (85–110 °C). Calcd for CuCN: 36.1. Found: 37.4 (110–130 °C).

(CuCN)₅(Py)₄, 1b. The procedure was identical to that used for **1a** except that the sample was vacuum dried overnight. A white powder was isolated (95.3%). IR (KBr pellet, cm⁻¹) 2125.5, 2101.2, 2086.0. Anal. Calcd for C₂₅H₂₀N₉Cu₅: C, 39.29; H, 2.64; N, 16.50. Found: C, 39.37; H, 2.61; N, 16.45. TGA Calcd for (CuCN)₂(Py): 84.5 Found: 82.8 (55–85 °C). Calcd for (CuCN)₄(Py): 71.5. Found: 71.4 (85–110 °C). Calcd for CuCN: 58.6. Found: 55.2 (110–130 °C).

(CuCN)₂(2-MePy)₃, 2a. The procedure was identical to that used for **1a**. A pale yellow powder was isolated (94.5%). IR (KBr pellet, cm⁻¹) 2128.1. Anal. Calcd for C₂₀H₂₁N₅Cu₂: C, 52.39; H, 4.62; N, 15.27. Found: C, 50.97; H, 4.40; N, 15.23. TGA Calcd for (CuCN)(2-MePy): 79.7 Found 80.9 (35–50 °C). Calcd for (CuCN)₂(2-MePy): 59.4 Found 60.3 (50–85 °C). Calcd for CuCN: 39.1 Found 40.3 (85–110 °C).

(CuCN)(2-MePy), 2b. The procedure was identical to that used for **1b**. A white powder was isolated (82.2%). IR (KBr pellet, cm⁻¹) 2127.7, 2102.2. Anal. Calcd for C₇H₇N₂Cu: C, 46.02; H, 3.86; N, 15.33. Found: C, 46.02; H, 3.69; N, 15.23. TGA Calcd for (CuCN)₂(2-MePy): 74.5. Found: 77.4 (50–85 °C). Calcd for CuCN: 49.0. Found: 51.4 (85–110 °C).

(CuCN)₂(3-MePy)₃, 3a. The procedure was identical to that used for **1a**. A straw-colored powder was isolated (95.5%). IR (KBr pellet, cm⁻¹) 2127.7, 2102.2. Anal. Calcd for C₂₀H₂₁N₅Cu₂: C, 52.39; H, 4.62; N, 15.27. Found: C, 52.37; H, 4.61; N, 14.99. TGA Calcd for (CuCN)(3-MePy): 79.7 Found 75.0 (30–50 °C). Calcd for (CuCN)₂(3-MePy): 54.7 Found 56.6 (50–90 °C). Calcd for CuCN: 39.1 Found 36.8 (90–130 °C).

(CuCN)(3-MePy), 3b. The procedure was identical to that used for **1b**. An off-white powder was isolated (81.4%). IR (KBr pellet, cm⁻¹) 2124.2, 2112.3, 2087.3. Anal. Calcd

for C₇H₇N₂Cu: C, 46.02; H, 3.86; N, 15.33. Found: C, 45.25; H, 3.79; N, 15.20. TGA Calcd for (CuCN)₂(2-MePy): 74.5. Found: 76.0 (60–100 °C). Calcd for CuCN: 49.0. Found: 50.2 (100–140 °C).

(CuCN)₂(4-MePy)₃, 4. The procedure was identical to that used for **1a**. A pale yellow powder was isolated (100%). IR (KBr pellet, cm⁻¹) 2114.9, 2100.5. Anal. Calcd for C₂₀H₂₁N₅Cu₂: C, 52.39; H, 4.62; N, 15.27. Found: C, 52.09; H, 4.58; N, 15.21. TGA Calcd for (CuCN)(4-MePy): 79.7 Found 79.8 (60–85 °C). Calcd for (CuCN)₂(4-MePy): 54.7 Found 59.5 (85–105 °C). Calcd for CuCN: 39.1 Found 39.3 (105–145 °C).

(CuCN)(2-EtPy), 5. The procedure was identical to that used for **1a**. A white powder was isolated (100%). IR (KBr pellet, cm⁻¹) 2127.5. Anal. Calcd for C₈H₉N₂Cu: C, 48.85; H, 4.61; N, 14.24. Found: C, 48.65; H, 4.49; N, 14.19. TGA Calcd for (CuCN)₂(2-EtPy): 74.5. Found: 77.4 (50–85 °C). Calcd for CuCN: 45.5. Found: 45.9 (65–105 °C).

(CuCN)₂(3-EtPy)₃, 6a. The procedure was similar to that used for **1a**. In this case a solution was quickly formed in the 3-EtPy. Once the solution had formed (30 min.), the mixture was cooling, causing spontaneous crystallization of the product. A pale yellow powder was isolated (94.4%). IR (KBr pellet, cm⁻¹) 2119.4, 2106.3. Anal. Calcd for C₂₃H₂₇N₅Cu₂: C, 55.19; H, 5.44; N, 13.99. Found: C, 55.08; H, 5.44; N, 13.97. TGA Calcd for (CuCN)₂(3-EtPy): 57.2 Found 58.9 (45–105 °C). Calcd for (CuCN)₄(3-EtPy): 46.5 Found 48.7 (105–240 °C). Calcd for CuCN: 35.8 Found 37.7 (240–300 °C).

(CuCN)(3-EtPy), 6b. The procedure was identical to that used for **1b**. A white powder was isolated (99.5%). IR (KBr pellet, cm⁻¹) 2125.1, 2106.7. Anal. Calcd for C₈H₉N₂Cu: C, 48.85; H, 4.61; N, 14.24. Found: C, 49.06; H, 4.66; N, 13.95. TGA Calcd for CuCN: 45.5. Found: 47.5 (90–125 °C).

(CuCN)(4-EtPy), 7. The procedure was identical to that used for **1a**. In this case a solution was formed in the 4-EtPy. This required addition of Et₂O to precipitate the product. A tan powder was isolated (77.4%). IR (KBr pellet, cm⁻¹) 2129.8, 2122.5. Anal. Calcd for C₈H₉N₂Cu: C, 48.85; H, 4.61; N, 14.24. Found: C, 48.03; H, 4.47; N, 14.08. TGA Calcd for (CuCN)₄(4-EtPy)₃: 86.4 Found 86.2 (60–110 °C). Calcd for (CuCN)₄(4-EtPy): 59.1 Found 62.0 (110–150 °C). Calcd for CuCN: 45.5 Found 47.5 (150–300 °C).

(CuCN)₂(4-*t*BuPy)₃, 8. The procedure was identical to that used for **1a**. A yellow crystalline solid was isolated (94.7%). When the same reaction was carried out with stirring, a white powder that gave identical analytical data was obtained (89.7%). IR (KBr pellet, cm⁻¹) 2123.6. Anal. Calcd for C₂₃H₂₇N₅Cu₂: C, 55.19; H, 5.44; N, 13.99. Found: C, 55.08; H, 5.44; N, 13.97. TGA Calcd for (CuCN)₂(4-*t*BuPy): 57.2 Found 58.9 (45–105 °C). Calcd for (CuCN)₄(4-*t*BuPy): 46.5 Found 48.7 (105–240 °C). Calcd for CuCN: 35.8 Found 34.5 (240–315 °C).

(CuCN)₃(Pipd)₄, 9. The procedure was identical to that used for **1a**. A white powder was isolated (97.6%). IR (KBr pellet, cm⁻¹) 2119.8, 2104.5, 2071.5. Anal. Calcd for C₁₈H₄₄N₇Cu₃: C, 45.34; H, 7.28; N, 16.09. Found: C, 44.61; H, 7.16; N, 15.97. TGA Calcd for (CuCN)₃(Pipd)₂: 72.0 Found 75.0 (35–90 °C). Calcd for (CuCN)₃(Pipd): 58.1 Found 58.8 (90–215 °C). Calcd for CuCN: 44.1 Found 44.5 (215–270 °C).

(CuCN)(N-MePipd), 10. The procedure was identical to that used for **1a**. A pale yellow powder was isolated (99.3%). IR (KBr pellet, cm⁻¹) 2139.1, 2132.3. Anal. Calcd for C₇H₁₃N₂Cu: C, 44.55; H, 6.94; N, 14.84. Found: C, 43.83; H, 6.85; N, 14.99. TGA Calcd for (CuCN)₂(N-MePipd): 73.7 Found 70.2 (45–70 °C). Calcd for CuCN: 47.5 Found 49.5 (70–100 °C).

(CuCN)₄(N-EtPipd)₃, 11. The procedure was identical to that used for **1a**. An off-white powder was isolated (97.5%). IR (KBr pellet, cm⁻¹) 2127.7. Anal. Calcd for C₂₅H₄₅N₇Cu₄: C, 43.03; H, 6.50; N, 14.05. Found: C, 43.14; H, 6.55; N, 13.91. TGA Calcd for (CuCN)₄(N-EtPipd): 67.6 Found 68.0 (55–90 °C). Calcd for CuCN: 51.3 Found 50.3 (90–105 °C).

(CuCN)(MeMorph), 12. The procedure was identical to that used for **1b**. A pale yellow powder was isolated (94.2%). IR (KBr pellet, cm⁻¹) 2119.8. Anal. Calcd for C₆H₁₁N₂OCu: C, 37.79; H, 5.81; N, 14.69. Found: C, 37.02; H, 5.73; N, 14.67. TGA Calcd for (CuCN)₃(MeMorph): 64.6 Found 63.3 (55–95 °C). Calcd for CuCN: 47.0 Found 47.3 (95–140 °C).

(CuCN)(Me₂NCy), 13. The procedure was identical to that used for **1a**. An off-white crystalline solid was isolated (93.7%). IR (KBr pellet, cm⁻¹) 2073.3. Anal. Calcd for C₉H₁₇N₂Cu: C, 49.86; H, 7.90; N, 12.92. Found: C, 49.96; H, 7.99; N, 12.76. TGA Calcd for (CuCN)₃(Me₂NCy): 60.9 Found 62.3 (45–80 °C). Calcd for CuCN: 42.2 Found 42.2 (75–110 °C).

General Method for Vapor Diffusion Reactions. About 80 mg CuCN powder or pressed pellet (prepared using an IR press) was placed in an uncapped 10 mL beaker. The beaker was placed in a small jar containing about 1-2 mL of liquid amine. After a few min. the CuCN luminescence reflected formation of the surface CuCN-amine phase.

X-ray Analysis. In some cases X-ray quality crystals were produced in the tube reactions described above. Single crystal determinations were carried out using a Bruker *SMART Apex II* diffractometer using graphite-monochromated Cu K α radiation.¹ Data for all complexes were collected at 100 K. The exception was complex **8**, which exhibited a

transition to a less orderly phase at around 230 K. Data for **8** were collected at room temperature. The data were corrected for Lorentz and polarization² effects and absorption using *SADABS*.³ The structures were solved by use of direct methods or Patterson map. Least squares refinement on F^2 was used for all reflections. Structure solution, refinement and the calculation of derived results were performed using the *SHELXTL*⁴ package of software. The non-hydrogen atoms were refined anisotropically. In all cases, hydrogen atoms were located then placed in theoretical positions. In most, but not all, cases the cyano C and N atoms were disordered. When required by crystallographic symmetry, occupancies of 50% C and 50% N were used; otherwise relative C and N occupancies were refined. Complex **13** ($P2_12_12_1$) was solved as a racemic twin, having Flack parameter of 0.53(2). For complexes **6a** and **8** disorder in the ethyl groups and the *t*-butyl groups, respectively, was modeled. For **6a** H atoms on C15 and C22 were only included for one of the two orientations of C16 and C23, respectively.

Powder diffraction analysis was carried out on the instrument described above as previously described⁵ or a Bruker D8 Advance instrument using a scan rate of 2°/min. covering 2–60° 2θ. The data were processed using *DIFFRAC-Plus* and *EVA* software.⁶ Simulated powder patterns from single crystal determinations were generated using the *Crystallographica* program.⁷

References:

1. *SMART Apex II, Data Collection Software*, version 2.1; Bruker AXS Inc.: Madison, WI, 2005.
2. *SAINT Plus, Data Reduction Software*, version 7.34a; Bruker AXS Inc.: Madison, WI, 2005.

3. G. M. Sheldrick, *SADABS*; University of Göttingen: Göttingen, Germany, 2005.
4. G. M. Sheldrick, *Acta Crystallogr., Sect. A* 2008, **64**, 112.
5. M. J. Lim, C. A. Murray, T. A. Tronic, K. E. deKrafft, A. N. Ley, J. C. deButts, R. D. Pike, H. Lu, H. H. Patterson, *Inorg. Chem.* 2008, **47**, 6931.
6. *DIFFRAC Plus*, version 10.0 and *EVA*, release 2004; Bruker AXS Inc.: Madison, WI, 2005.
7. *Crystallographica*, version 1.60d; Oxford Cryosystems Ltd.: Oxford, U.K. 2007.

Figure S1. Luminescence photos of authentic $(\text{CuCN})\text{L}_n$ samples (neat, heated) under 254 nm irradiation. **1a** ($\text{CuCN})(\text{Py})_2$, **1b** ($\text{CuCN})_5(\text{Py})_4$, **2a** ($\text{CuCN})_2(2\text{-MePy})_3$, **2b** ($\text{CuCN})(2\text{-MePy})3a ($\text{CuCN})_2(3\text{-MePy})_3$, **3b** ($\text{CuCN})(3\text{-MePy})$, **4** ($\text{CuCN})_2(4\text{-MePy})_3$, **5** ($\text{CuCN})(2\text{-EtPy})6a ($\text{CuCN})_2(3\text{-EtPy})_3$, **6b** ($\text{CuCN})(3\text{-EtPy})$, **7** ($\text{CuCN})(4\text{-EtPy})$, **8** ($\text{CuCN})_2(4\text{-}^{\prime}\text{BuPy})_3$, **9** ($\text{CuCN})_3(\text{Pipd})_4$, **10** ($\text{CuCN})(\text{N-MePipd})$, **11** ($\text{CuCN})_4(\text{N-EtPipd})_3$, **12** ($\text{CuCN})(\text{N-MeMorph})$, **13** ($\text{CuCN})(\text{Me}_2\text{NCy})$$$

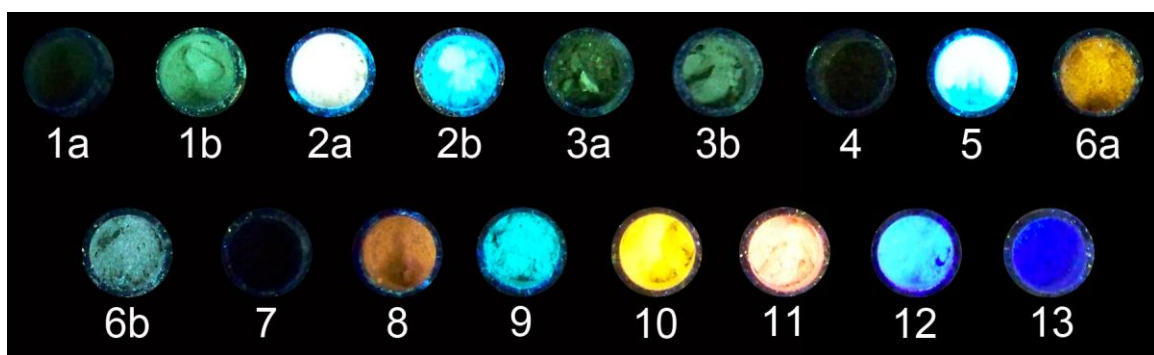


Table S1. Crystal data and structure refinement for **2b**.

Identification code	p21onc
Empirical formula	C7 H7 Cu N2
Formula weight	182.69
Temperature	100(2) K
Wavelength	1.54178 Å
Crystal system	Monoclinic
Space group	P2(1)/c
Unit cell dimensions	$a = 10.0593(2)$ Å $\alpha = 90^\circ$. $b = 8.72760(10)$ Å $\beta = 108.7090(10)^\circ$. $c = 8.9901(2)$ Å $\gamma = 90^\circ$.
Volume	747.57(2) Å ³
Z	4
Density (calculated)	1.623 Mg/m ³
Absorption coefficient	3.451 mm ⁻¹
F(000)	368
Crystal size	0.32 x 0.12 x 0.08 mm ³
Theta range for data collection	4.64 to 66.99°.
Index ranges	-11≤h≤11, -9≤k≤10, -10≤l≤8
Reflections collected	7274
Independent reflections	1273 [R(int) = 0.0362]
Completeness to theta = 66.99°	95.7 %
Absorption correction	Numerical
Max. and min. transmission	0.7603 and 0.4010
Refinement method	Full-matrix least-squares on F ²
Data / restraints / parameters	1273 / 0 / 93
Goodness-of-fit on F ²	1.098
Final R indices [I>2sigma(I)]	R1 = 0.0276, wR2 = 0.0768
R indices (all data)	R1 = 0.0316, wR2 = 0.0791
Largest diff. peak and hole	0.537 and -0.363 e.Å ⁻³

Table S2. Crystal data and structure refinement for **6a**.

Identification code	p212121	
Empirical formula	C ₂₃ H ₂₇ Cu ₂ N ₅	
Formula weight	500.58	
Temperature	100(2) K	
Wavelength	1.54178 Å	
Crystal system	Orthorhombic	
Space group	P2(1)2(1)2(1)	
Unit cell dimensions	a = 8.6557(2) Å	α = 90°.
	b = 16.5520(4) Å	β = 90°.
	c = 17.2948(4) Å	γ = 90°.
Volume	2477.81(10) Å ³	
Z	4	
Density (calculated)	1.342 Mg/m ³	
Absorption coefficient	2.242 mm ⁻¹	
F(000)	1032	
Crystal size	0.36 x 0.35 x 0.15 mm ³	
Theta range for data collection	3.70 to 67.00°.	
Index ranges	-9<=h<=10, -19<=k<=17, -20<=l<=19	
Reflections collected	26626	
Independent reflections	4362 [R(int) = 0.0362]	
Completeness to theta = 67.00°	99.1 %	
Absorption correction	Numerical	
Max. and min. transmission	0.7326 and 0.4958	
Refinement method	Full-matrix least-squares on F ²	
Data / restraints / parameters	4362 / 0 / 291	
Goodness-of-fit on F ²	1.063	
Final R indices [I>2sigma(I)]	R1 = 0.0217, wR2 = 0.0573	
R indices (all data)	R1 = 0.0219, wR2 = 0.0574	
Absolute structure parameter	0.004(19)	
Largest diff. peak and hole	0.650 and -0.389 e.Å ⁻³	

Table S3. Crystal data and structure refinement for **8**.

Identification code	fdd2	
Empirical formula	C29 H39 Cu2 N5	
Formula weight	584.73	
Temperature	296(2) K	
Wavelength	1.54178 Å	
Crystal system	orthorhombic	
Space group	Fdd2	
Unit cell dimensions	a = 14.9500(2) Å b = 35.3082(4) Å c = 11.64710(10) Å	α= 90°. β= 90°. γ = 90°.
Volume	6148.01(12) Å ³	
Z	8	
Density (calculated)	1.263 Mg/m ³	
Absorption coefficient	1.879 mm ⁻¹	
F(000)	2448	
Crystal size	0.35 x 0.23 x 0.21 mm ³	
Theta range for data collection	4.97 to 66.93°.	
Index ranges	-16<=h<=17, -41<=k<=42, -12<=l<=13	
Reflections collected	16270	
Independent reflections	2594 [R(int) = 0.0307]	
Completeness to theta = 66.93°	96.9 %	
Max. and min. transmission	0.6982 and 0.5626	
Refinement method	Full-matrix least-squares on F ²	
Data / restraints / parameters	2594 / 122 / 193	
Goodness-of-fit on F ²	0.942	
Final R indices [I>2sigma(I)]	R1 = 0.0311, wR2 = 0.0916	
R indices (all data)	R1 = 0.0325, wR2 = 0.0934	
Absolute structure parameter	0.02(5)	
Largest diff. peak and hole	0.172 and -0.261 e.Å ⁻³	

Table S4. Crystal data and structure refinement for **9**.

Identification code	c2onc		
Empirical formula	C23 H44 Cu3 N7		
Formula weight	609.27		
Temperature	100(2) K		
Wavelength	1.54178 Å		
Crystal system	Monoclinic		
Space group	C2/c		
Unit cell dimensions	$a = 26.3331(2)$ Å	$\alpha = 90^\circ$.	
	$b = 5.22920(10)$ Å	$\beta = 122.6785(3)^\circ$.	
	$c = 23.7064(2)$ Å	$\gamma = 90^\circ$.	
Volume	$2747.68(6)$ Å ³		
Z	4		
Density (calculated)	1.473 Mg/m ³		
Absorption coefficient	2.870 mm ⁻¹		
F(000)	1272		
Crystal size	0.24 x 0.08 x 0.03 mm ³		
Theta range for data collection	3.99 to 66.98°.		
Index ranges	-30≤h≤31, -6≤k≤5, -27≤l≤27		
Reflections collected	14544		
Independent reflections	2413 [R(int) = 0.0311]		
Completeness to theta = 66.98°	98.6 %		
Absorption correction	Numerical		
Max. and min. transmission	0.9188 and 0.5458		
Refinement method	Full-matrix least-squares on F ²		
Data / restraints / parameters	2413 / 0 / 239		
Goodness-of-fit on F ²	1.016		
Final R indices [I>2sigma(I)]	R1 = 0.0212, wR2 = 0.0582		
R indices (all data)	R1 = 0.0229, wR2 = 0.0594		
Largest diff. peak and hole	0.529 and -0.226 e.Å ⁻³		

Table S5. Crystal data and structure refinement for **12**.

Identification code	ama2	
Empirical formula	C ₆ H ₁₁ CuN ₂ O	
Formula weight	190.71	
Temperature	100(2) K	
Wavelength	1.54178 Å	
Crystal system	Orthorhombic	
Space group	Ama2	
Unit cell dimensions	a = 9.7119(2) Å b = 12.2714(3) Å c = 6.2836(2) Å	α = 90°. β = 90°. γ = 90°.
Volume	748.87(3) Å ³	
Z	4	
Density (calculated)	1.691 Mg/m ³	
Absorption coefficient	3.561 mm ⁻¹	
F(000)	392	
Crystal size	0.20 x 0.11 x 0.06 mm ³	
Theta range for data collection	7.22 to 66.82°.	
Index ranges	-10<=h<=11, -13<=k<=14, -6<=l<=7	
Reflections collected	3902	
Independent reflections	661 [R(int) = 0.0352]	
Completeness to theta = 66.82°	100.0 %	
Absorption correction	Numerical	
Max. and min. transmission	0.8147 and 0.5347	
Refinement method	Full-matrix least-squares on F ²	
Data / restraints / parameters	661 / 1 / 52	
Goodness-of-fit on F ²	1.107	
Final R indices [I>2sigma(I)]	R1 = 0.0175, wR2 = 0.0403	
R indices (all data)	R1 = 0.0180, wR2 = 0.0406	
Absolute structure parameter	0.03(4)	
Largest diff. peak and hole	0.216 and -0.236 e.Å ⁻³	

Table S6. Crystal data and structure refinement for **13**.

Identification code	p212121		
Empirical formula	C9 H17 Cu N2		
Formula weight	216.79		
Temperature	100(2) K		
Wavelength	1.54178 Å		
Crystal system	Monoclinic		
Space group	P2(1)2(1)2(1)		
Unit cell dimensions	$a = 6.31450(10)$ Å	$\alpha = 90^\circ$.	
	$b = 9.34500(10)$ Å	$\beta = 90^\circ$.	
	$c = 17.4458(3)$ Å	$\gamma = 90^\circ$.	
Volume	$1029.46(3)$ Å ³		
Z	4		
Density (calculated)	1.399 Mg/m ³		
Absorption coefficient	2.579 mm ⁻¹		
F(000)	456		
Crystal size	0.27 x 0.19 x 0.11 mm ³		
Theta range for data collection	5.07 to 67.00°.		
Index ranges	-6<=h<=7, -10<=k<=10, -20<=l<=20		
Reflections collected	10747		
Independent reflections	1814 [R(int) = 0.0280]		
Completeness to theta = 67.00°	98.8 %		
Absorption correction	Numerical		
Max. and min. transmission	0.7576 and 0.5427		
Refinement method	Full-matrix least-squares on F ²		
Data / restraints / parameters	1814 / 0 / 113		
Goodness-of-fit on F ²	1.154		
Final R indices [I>2sigma(I)]	R1 = 0.0164, wR2 = 0.0439		
R indices (all data)	R1 = 0.0165, wR2 = 0.0440		
Absolute structure parameter	0.53(2)		
Largest diff. peak and hole	0.277 and -0.167 e.Å ⁻³		

Table S7. Selected bond lengths (\AA) and angles ($^{\circ}$) for all complexes.^a

Complex 2b , $(\text{CuCN})(2\text{MePy})$			
Cu-X	1.888(2), 1.914(2)	X-Cu ^b -X	130.71(8)
X-X	1.168(3)	X-Cu ^b -N	108.61(7), 120.58(8)
Cu ^b -N	2.0444(19)	Cu-X-X	174.69(18), 178.1(2)
Complex 6a , $(\text{CuCN})_2(3\text{EtPy})_3$			
Cu-X	1.8713(18), 1.8911(19), 1.8936(17), 1.9720(16)	X-Cu ^b -X	144.99(7)
X-X	1.156(3), 1.160(2)	X-Cu ^c -X	127.45(7)
Cu ^b -N	2.0936(17)	X-Cu ^b -N	104.26(7), 110.71(7)
Cu ^c -N	2.1006(16), 2.1209(16)	X-Cu ^c -N	98.42(6), 102.35(7), 112.41(7), 112.41(7)
		N-Cu ^c -N	98.45(6)
		Cu-X-X	172.10(15), 176.56(15), 177.07(16), 179.35(17)
Complex 8 , $(\text{CuCN})_2(4'\text{BuPy})_3$			
Cu-X	1.882(3), 1.892(3)	X-Cu ^b -X	146.91(12)
X-X	1.149(4)	X-Cu ^b -N	105.40(11), 107.69(12)
Cu ^b -N	2.097(3)	Cu-X-X	175.2(3), 175.6(3)
Complex 9 , $(\text{CuCN})_3(\text{Pipd})_4$			
Cu-X	1.8691(15), 1.8962(15), 1.9196(15)	X-Cu ^b -X	143.51(6)
X-X	1.161(3), 1.164(2)	X-Cu ^c -X	125.27(9)
Cu ^b -N	2.1421(13)	X-Cu ^b -N	99.97(6), 116.48(6)
Cu ^c -N	2.1795(13)	X-Cu ^c -N	104.97(5), 111.78(5)

N-Cu^c-N 93.60(7)

Cu-X-X 175.28(13), 177.22(14), 179.19(18)

Complex **12**, (CuCN)(MeMorph)

Cu-X 1.9021(15) X-Cu^b-X 154.19(9)

X-X 1.157(3) X-Cu^b-N 102.07(6)

Cu^b-N 2.254(2) Cu-X-X 173.92(18)

Cu···O 2.537(3)

Complex **13**, (CuCN)(Me₂CyN)

Cu-X 1.8827(13), 1.8863(14) X-Cu^b-X 143.51(5)

X-X 1.157(2) X-Cu^b-N 107.05(5), 108.95(5)

Cu^b-N 2.1864(11) Cu-X-X 174.30(12), 178.24(13)

^aX indicates cyanide C/N, N indicates L ligand. ^b3-Coordinate Cu atom. ^c4-Coordinate Cu atom.

Figure S2. TGA for **1a**.

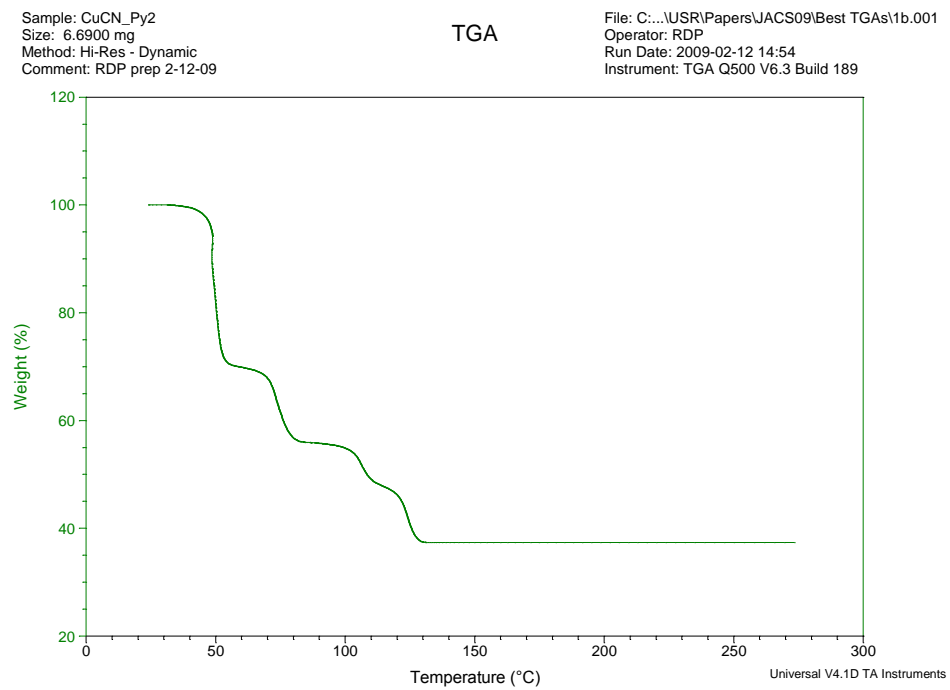


Figure S3. TGA for **1b**.

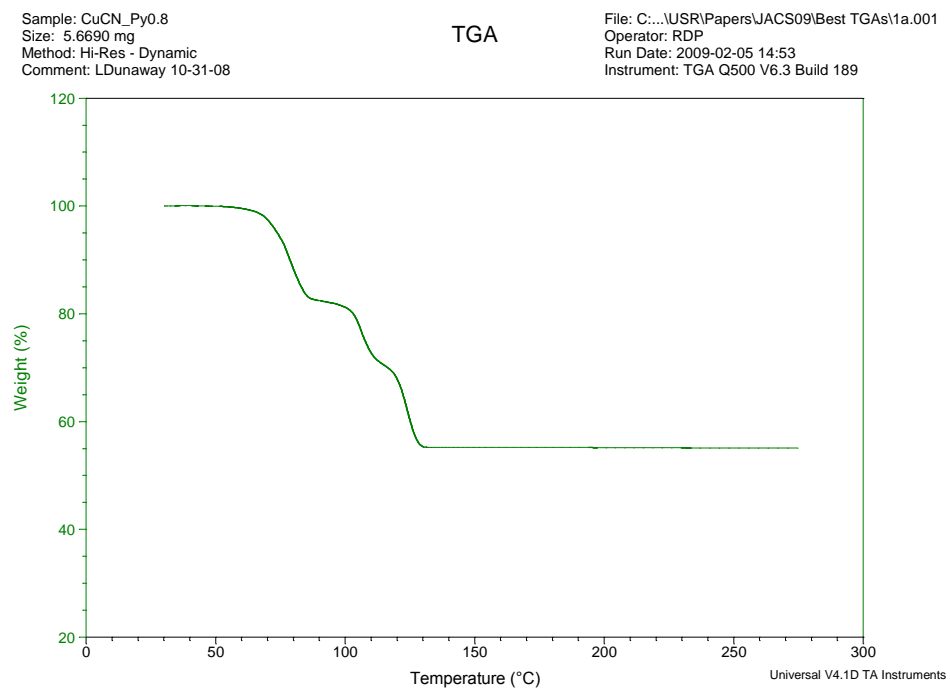


Figure S4. TGA for **2a**.

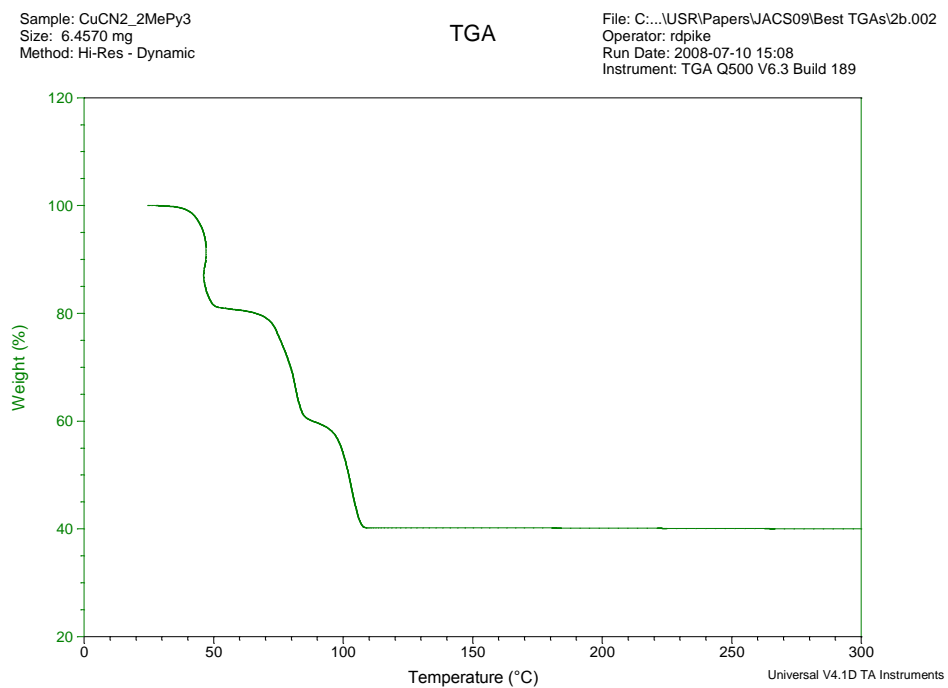


Figure S5. TGA for **2b**.

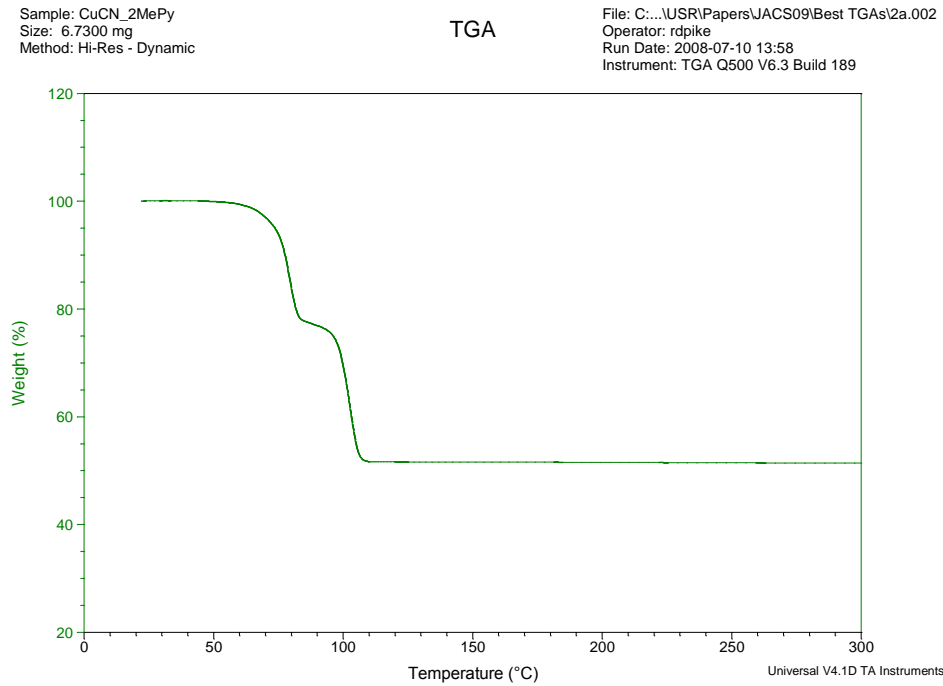


Figure S6. TGA for **3a**.

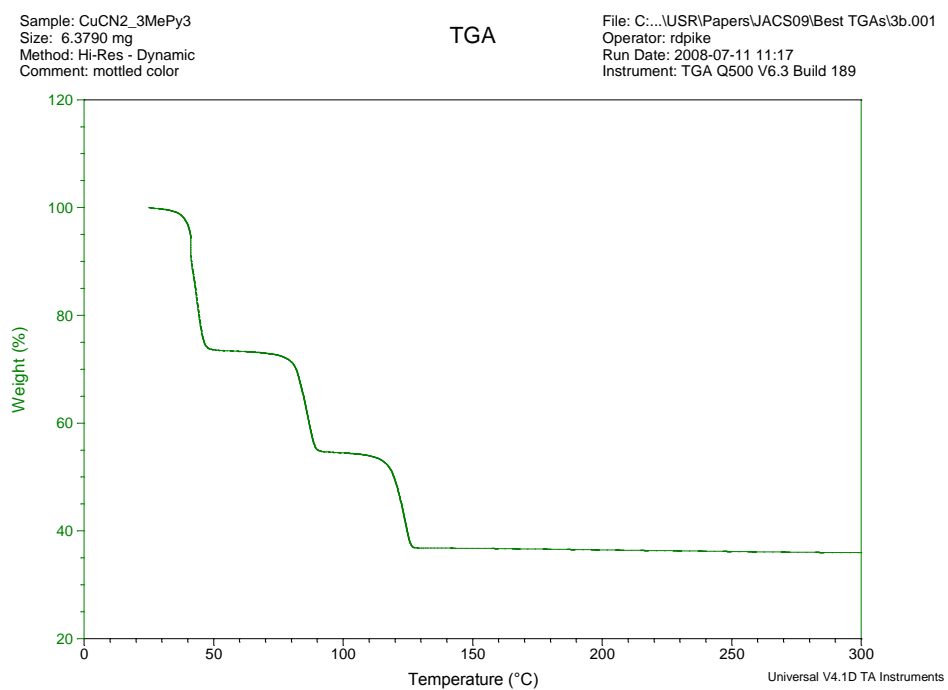


Figure S7. TGA for **3b**.

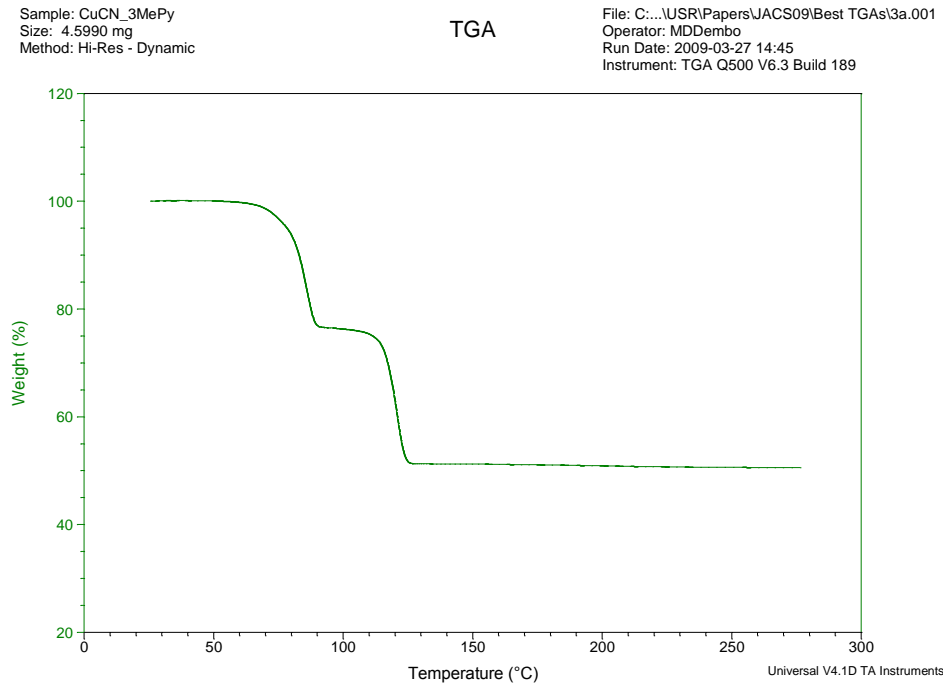


Figure S8. TGA for 4.

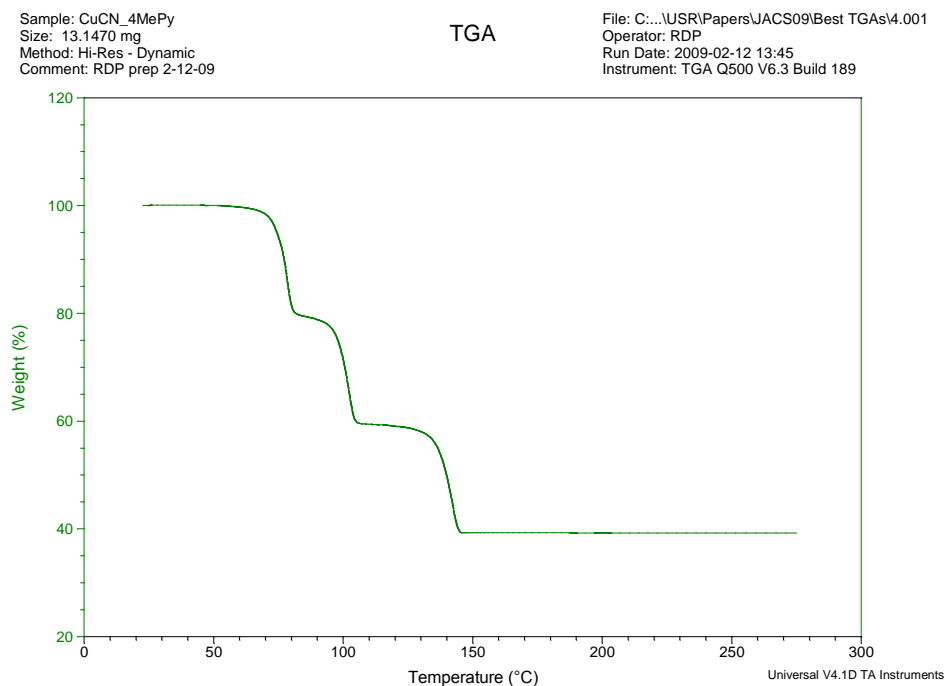


Figure S9. TGA for 5.

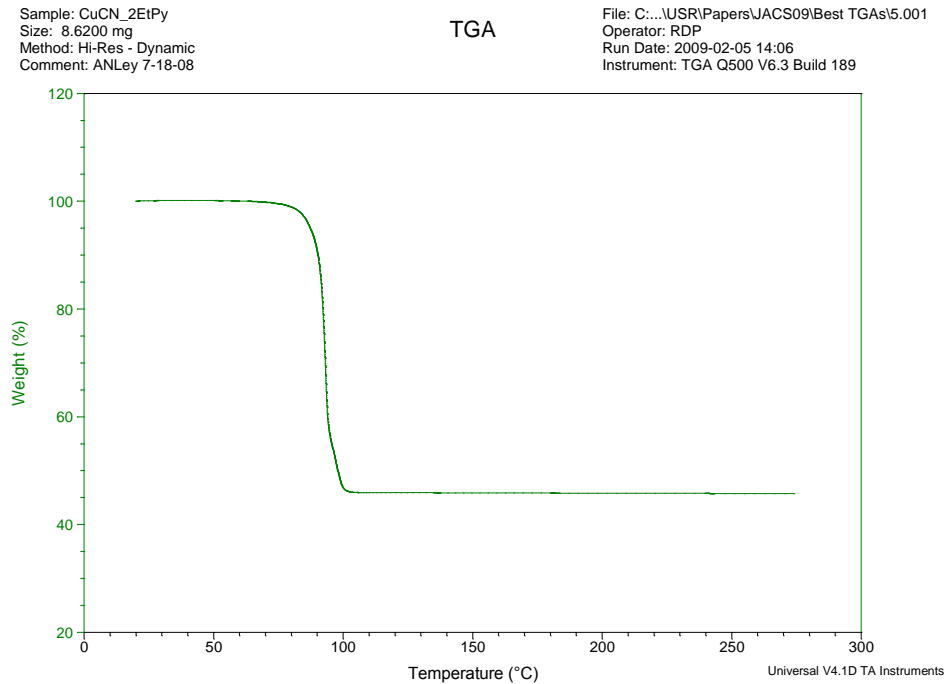


Figure S10. TGA for **6a**.

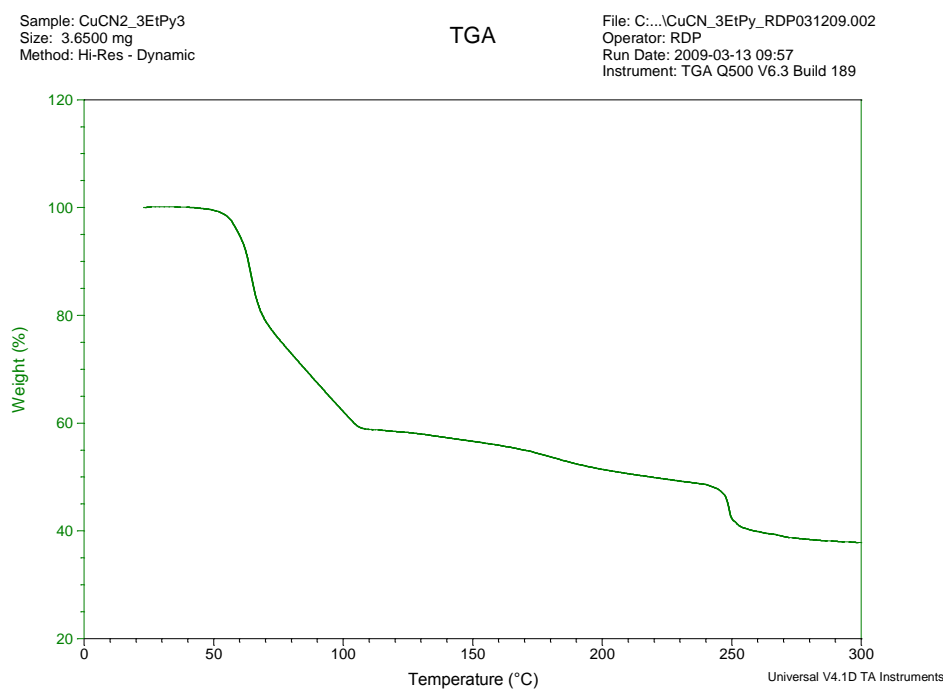


Figure S11. TGA for **6b**.

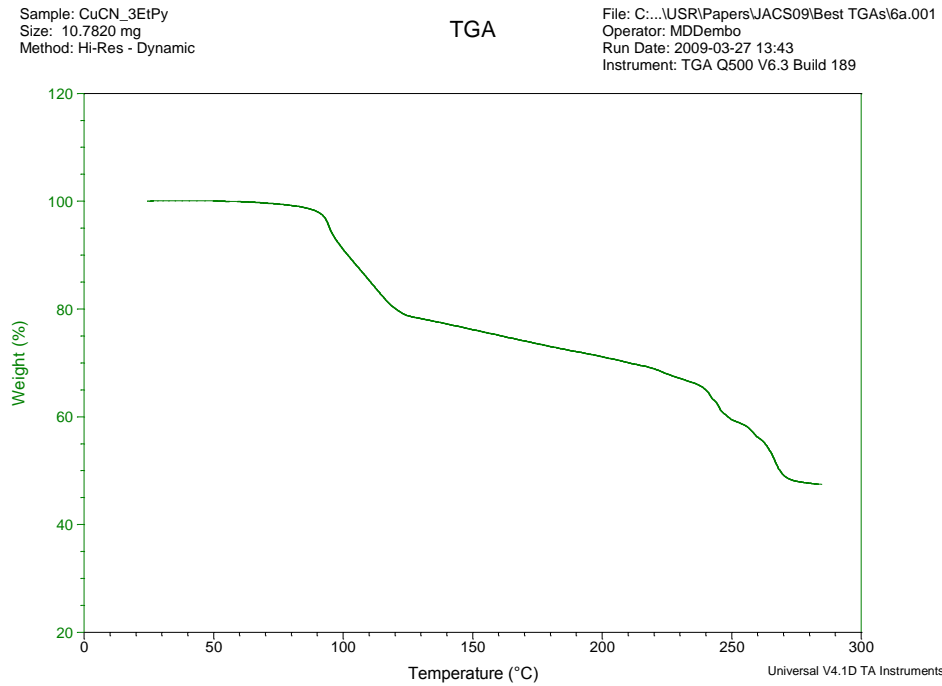


Figure S12. TGA for 7.

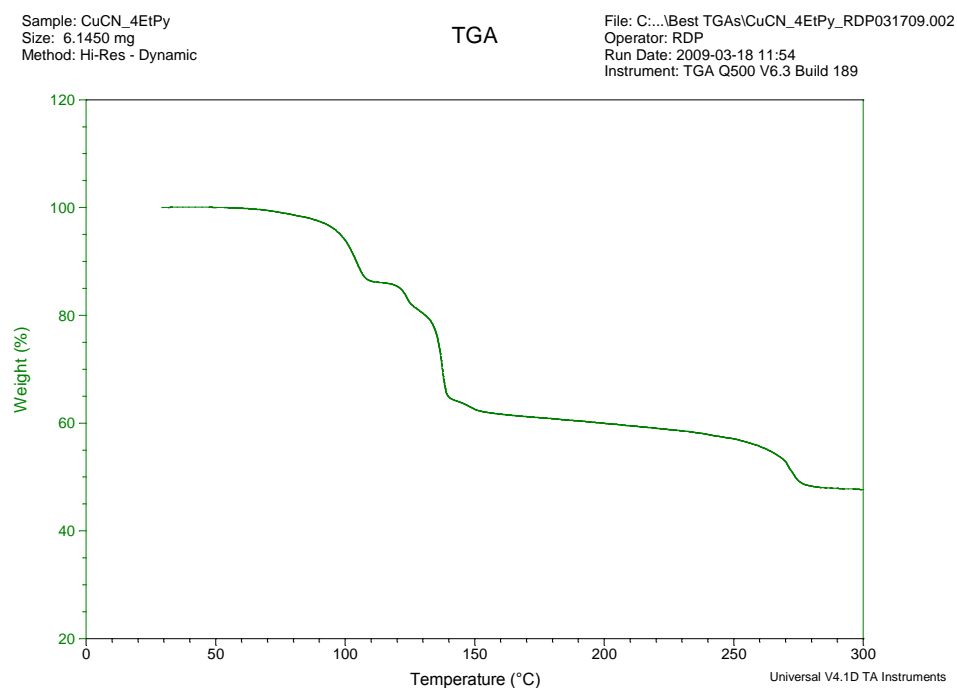


Figure S13. TGA for 8.

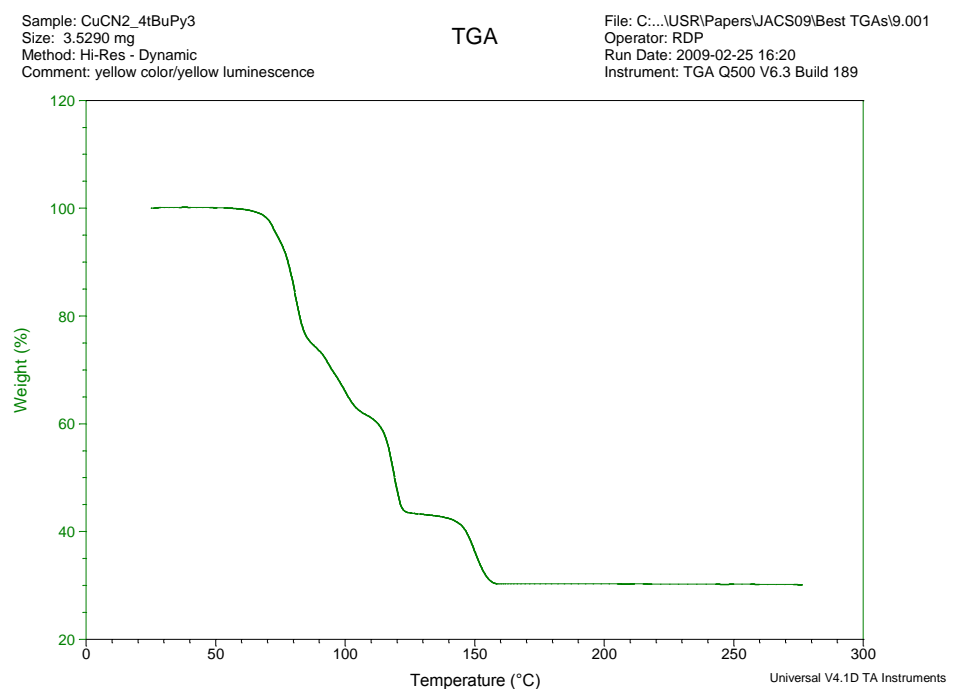


Figure S14. TGA for **9**.

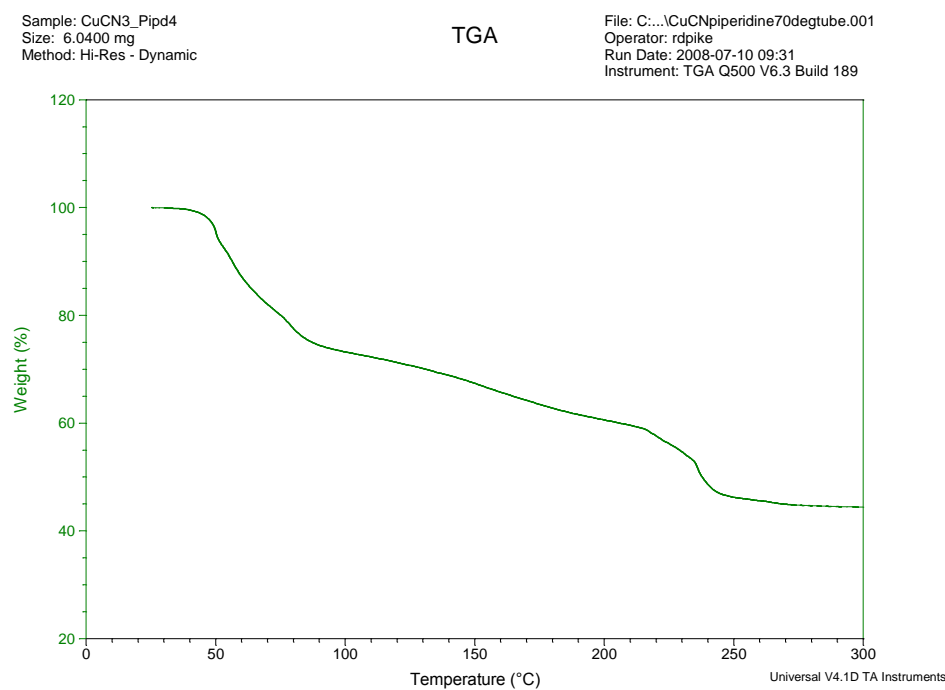


Figure S15. TGA for **10**.

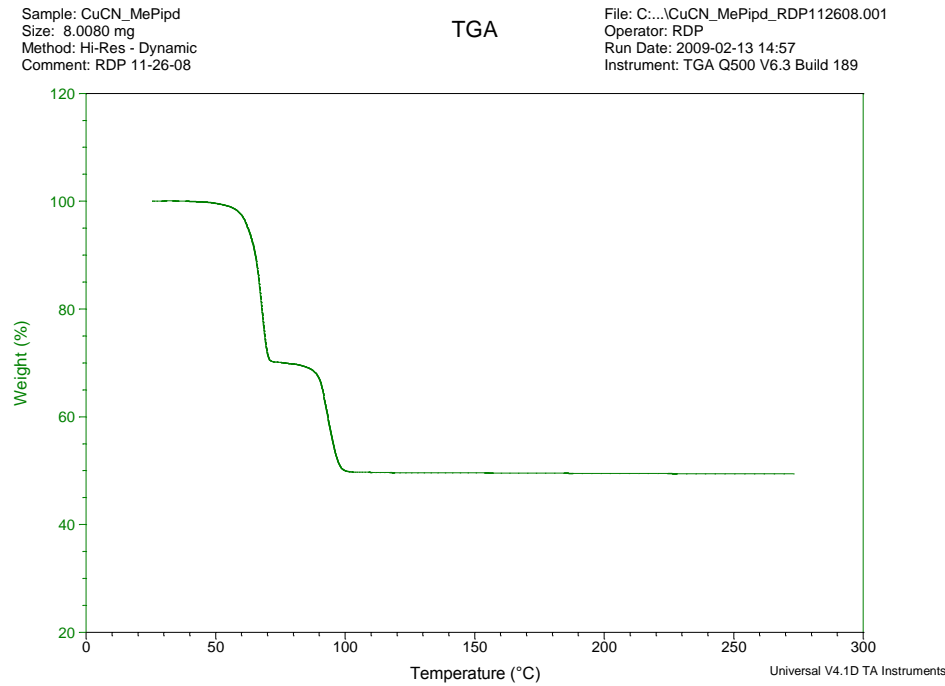


Figure S16. TGA for **11**.

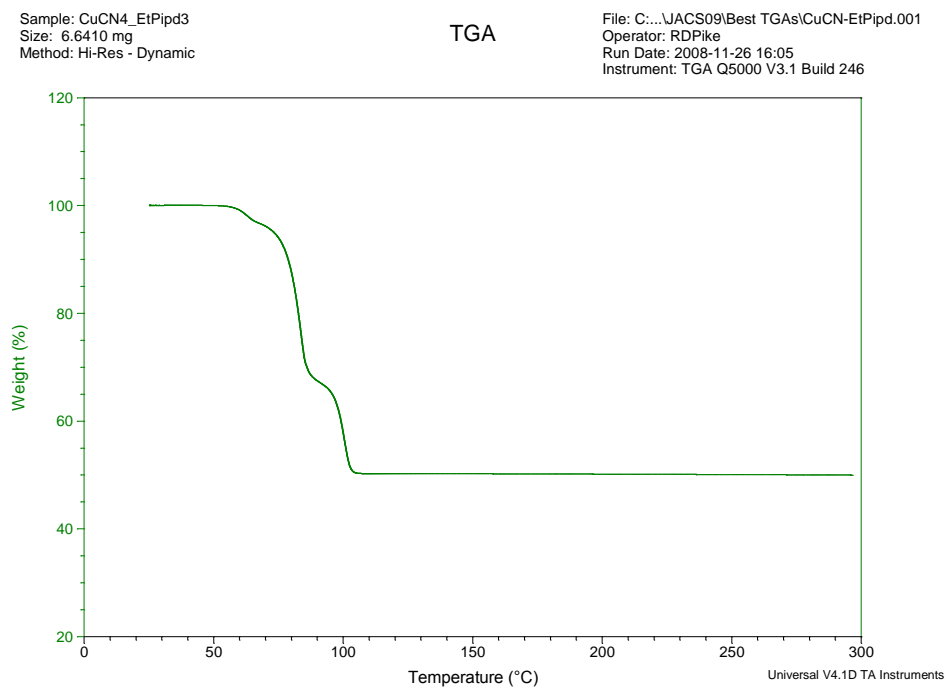


Figure S17. TGA for **12**.

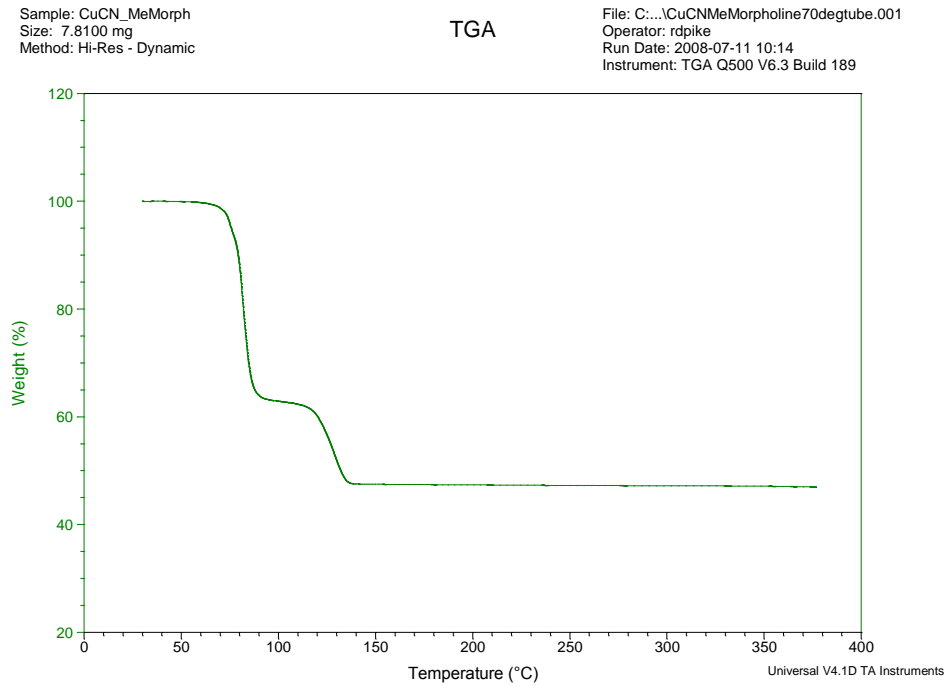


Figure S18. TGA for **13**.

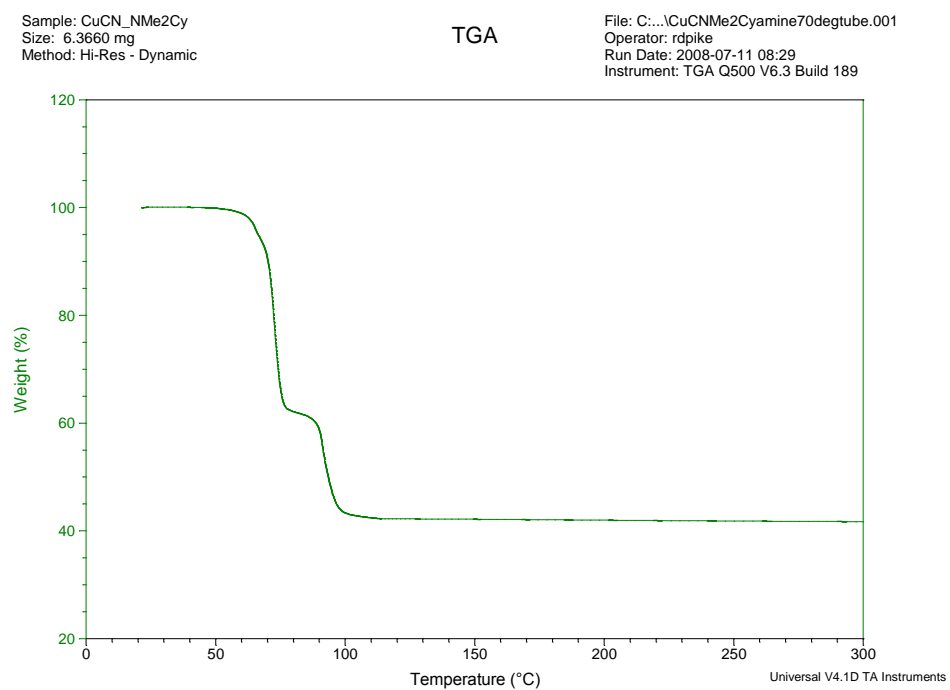


Figure S19. Powder diffractogram of CuCN.

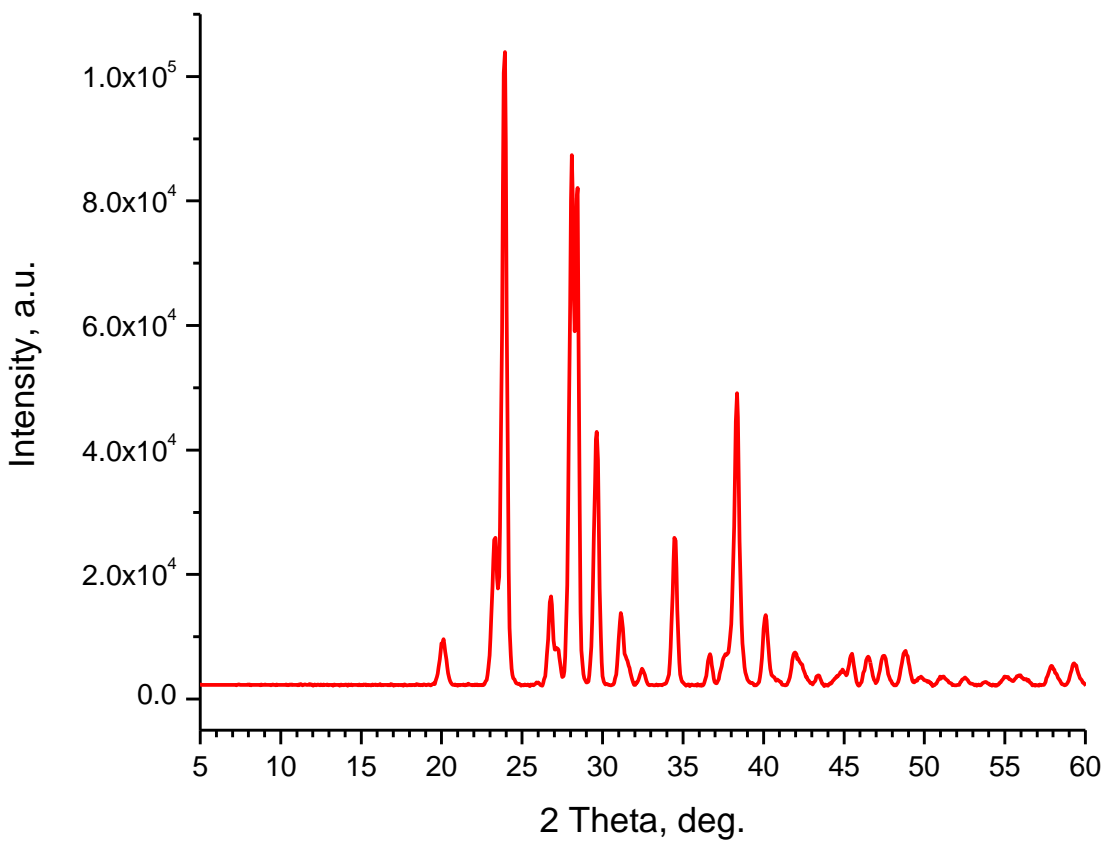


Figure S20. Experimental and calculated powder diffractograms of **1a**, (CuCN)(Py)₂.

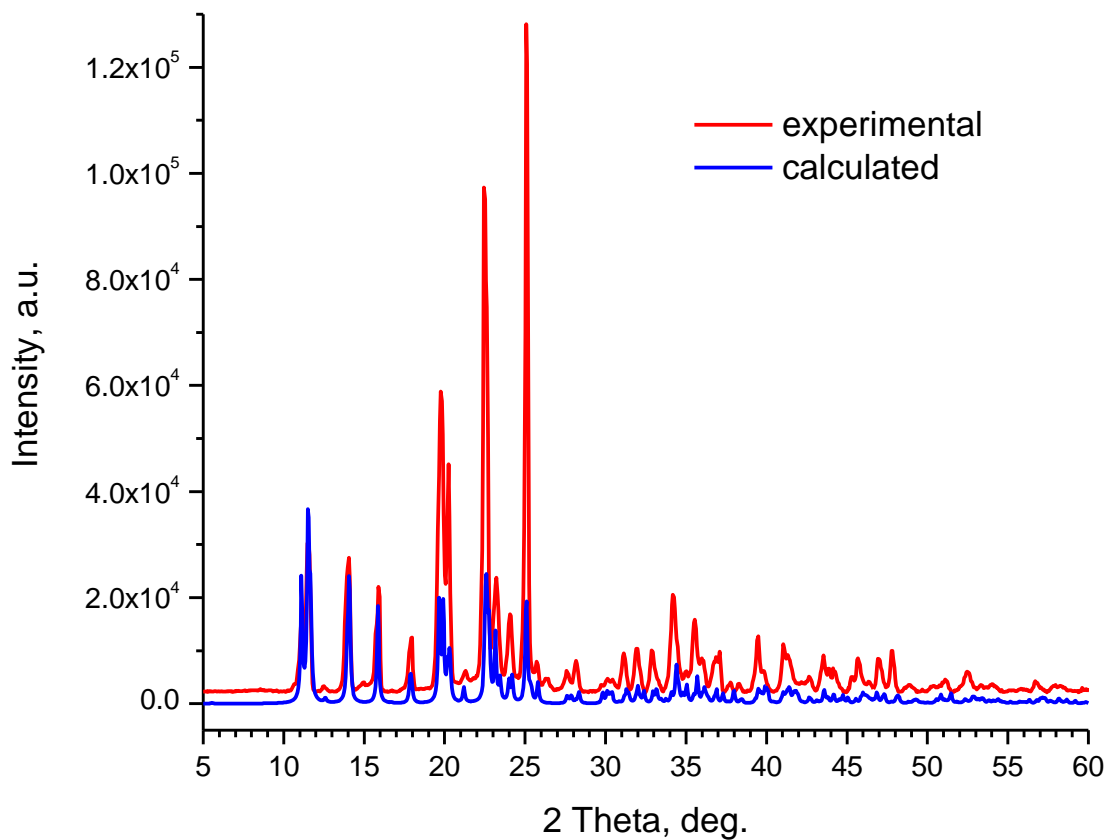


Figure S21. Powder diffractogram of **1b**, $(\text{CuCN})_5(\text{Py})_4$.

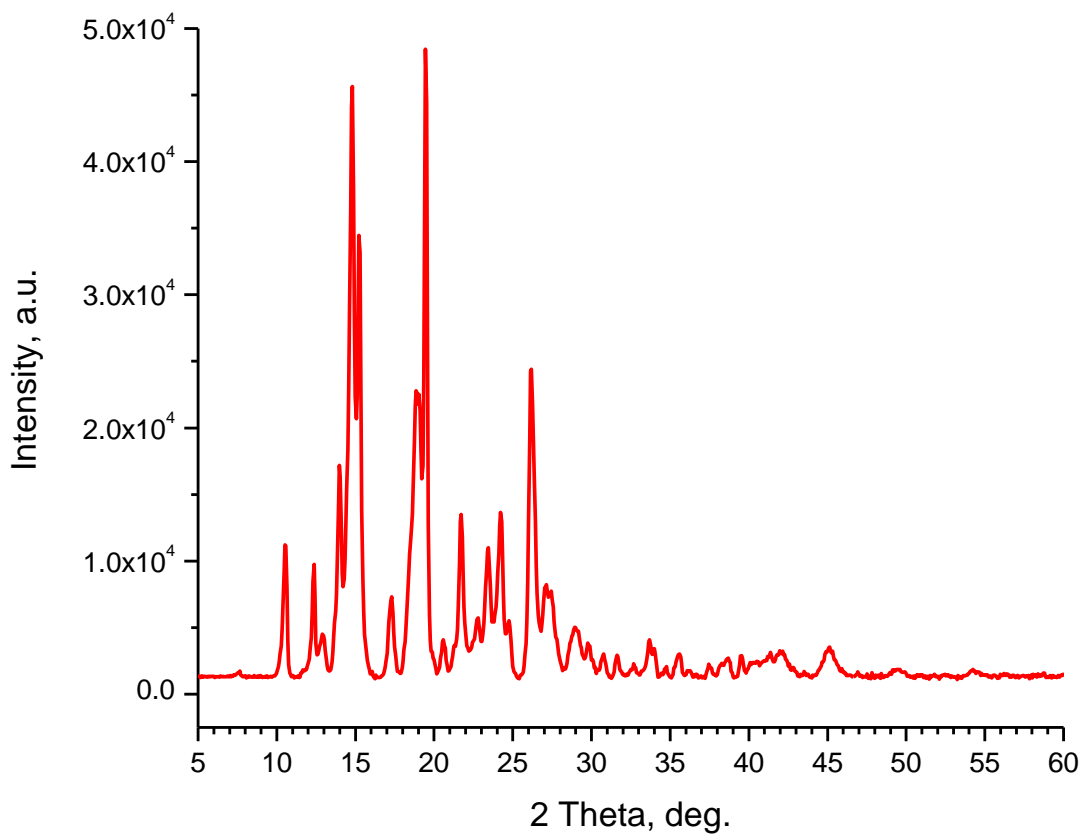


Figure S22. Experimental and calculated powder diffractograms of **2a**, $(\text{CuCN})_2(2\text{-MePy})_3$.

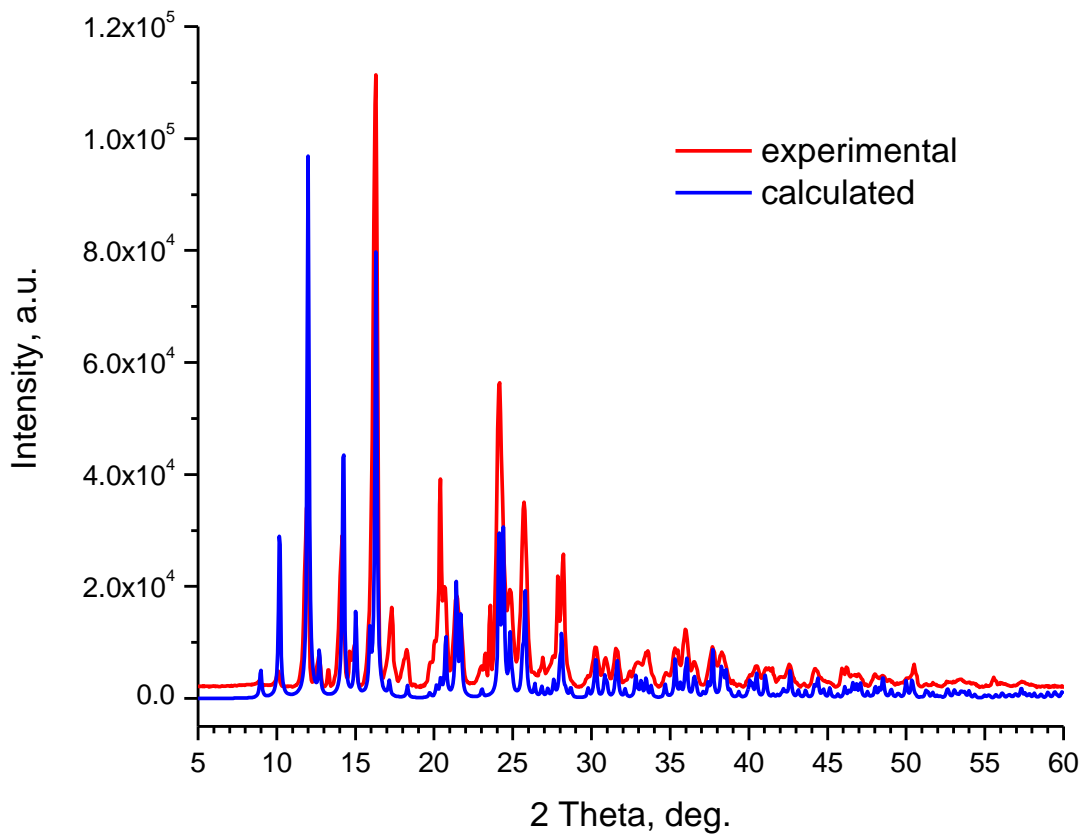


Figure S23. Experimental and calculated powder diffractograms of **2b**, (CuCN)(2-MePy).

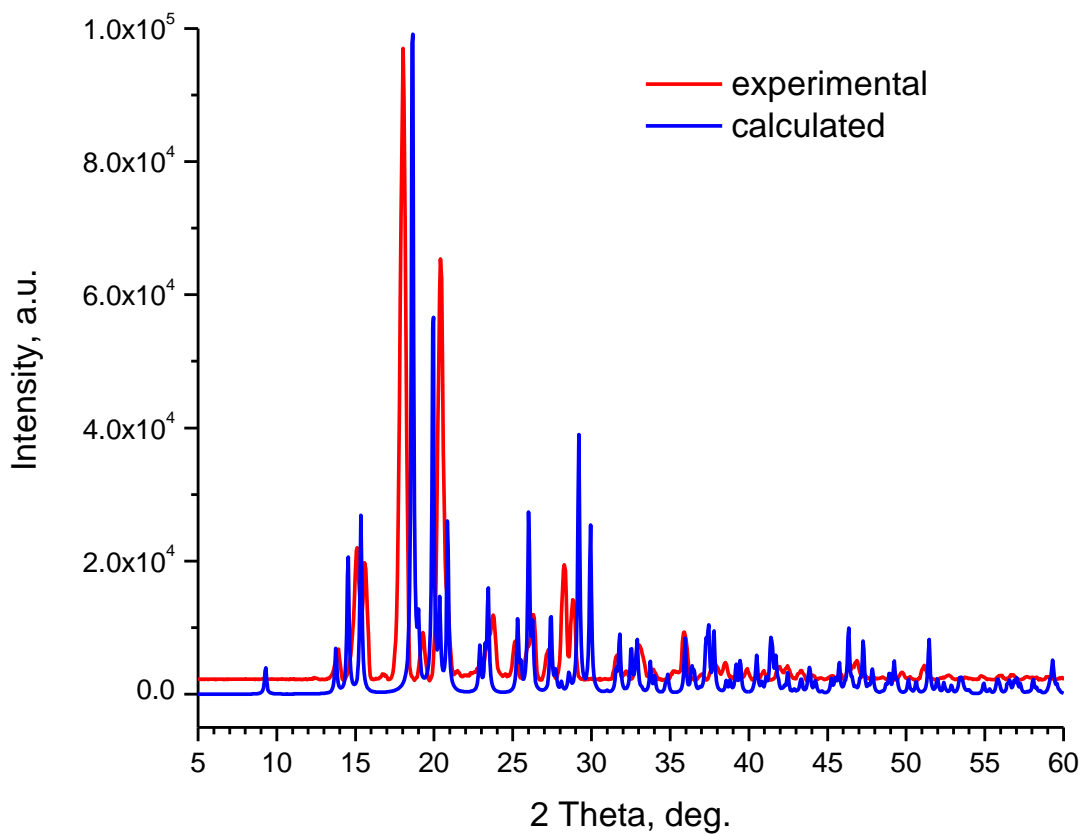


Figure S24. Powder diffractogram of **3a**, $(\text{CuCN})_2(3\text{-MePy})_3$.

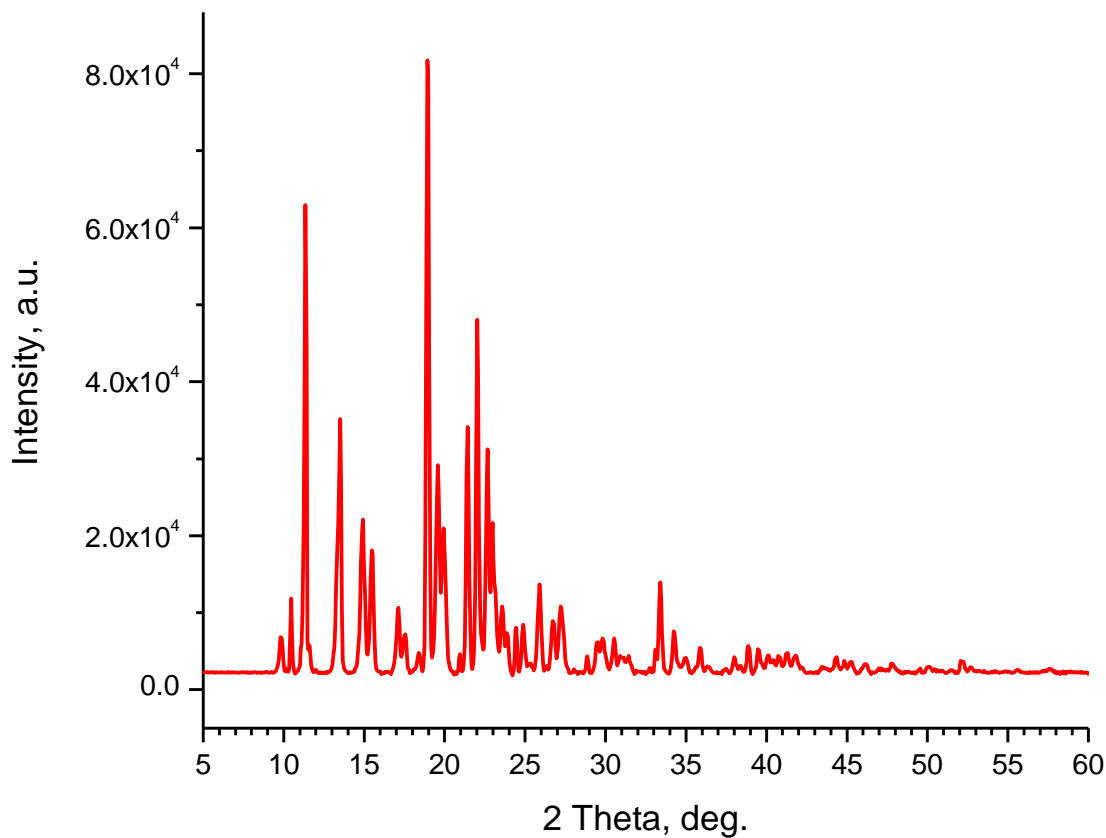


Figure S25. Powder diffractogram of **3b**, (CuCN)(3-MePy).

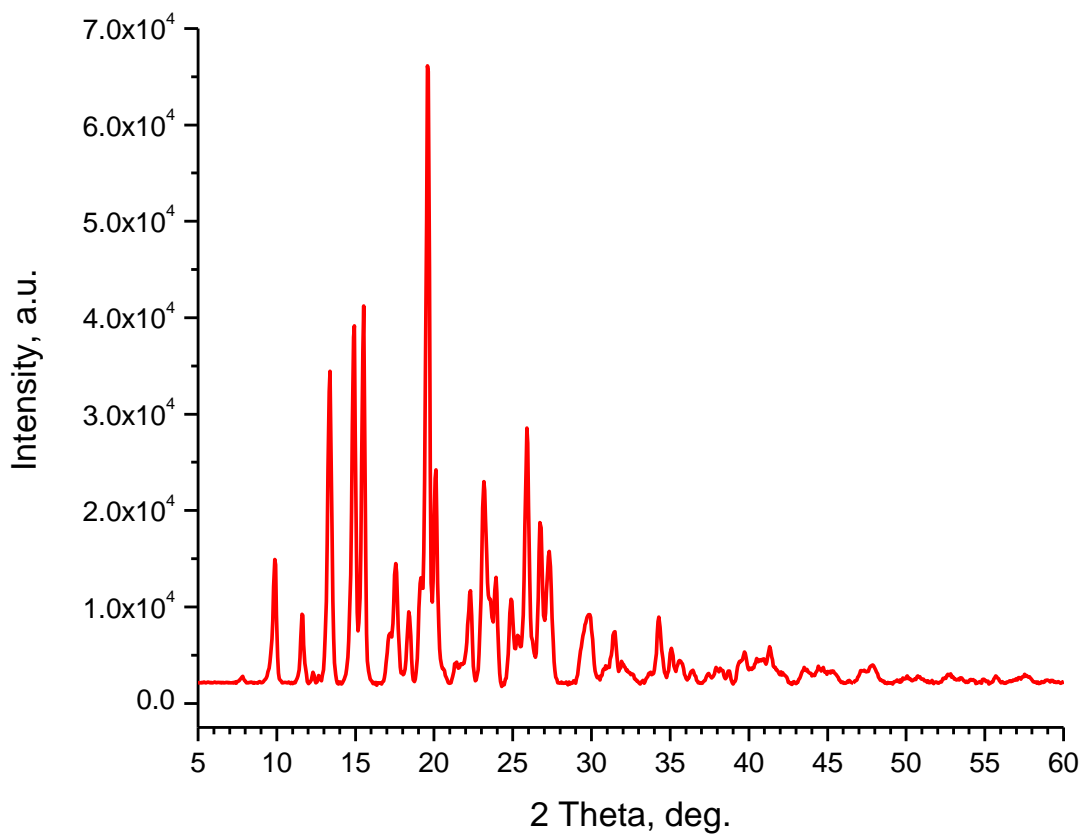


Figure S26. Experimental and calculated powder diffractograms of **4**, $(\text{CuCN})_2(4\text{-MePy})_3$.

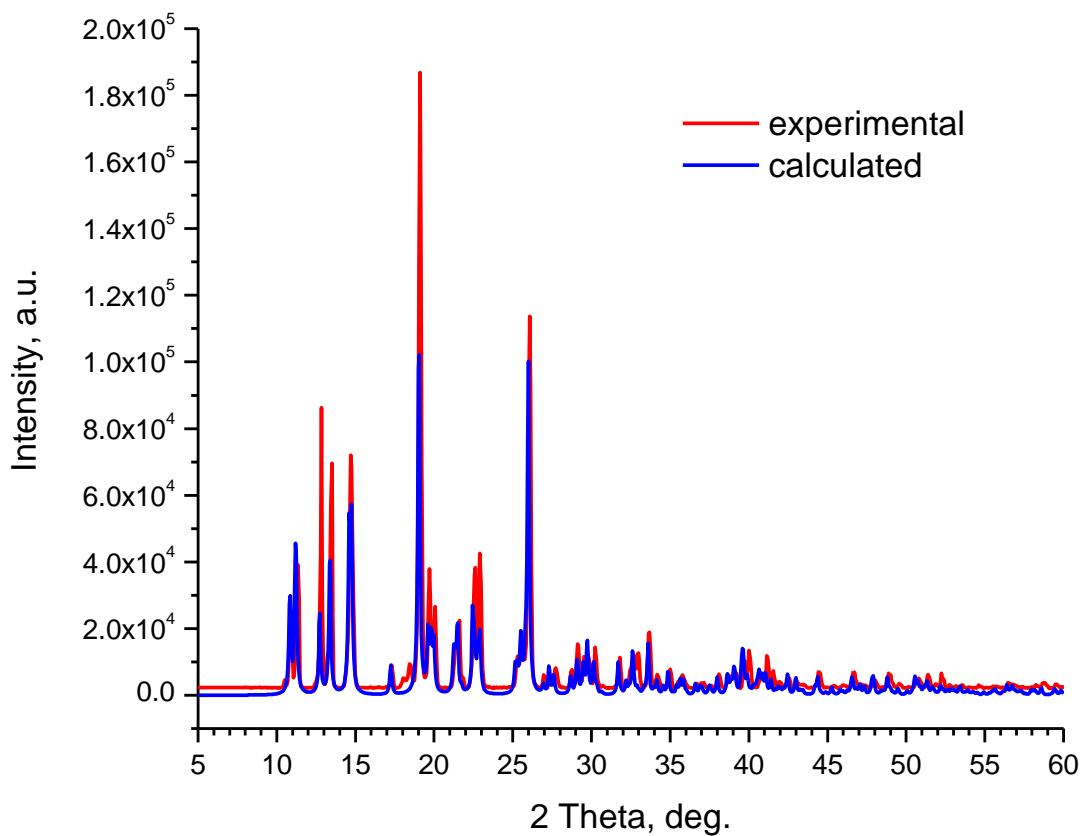


Figure S27. Powder diffractogram of **5**, (CuCN)(2-EtPy).

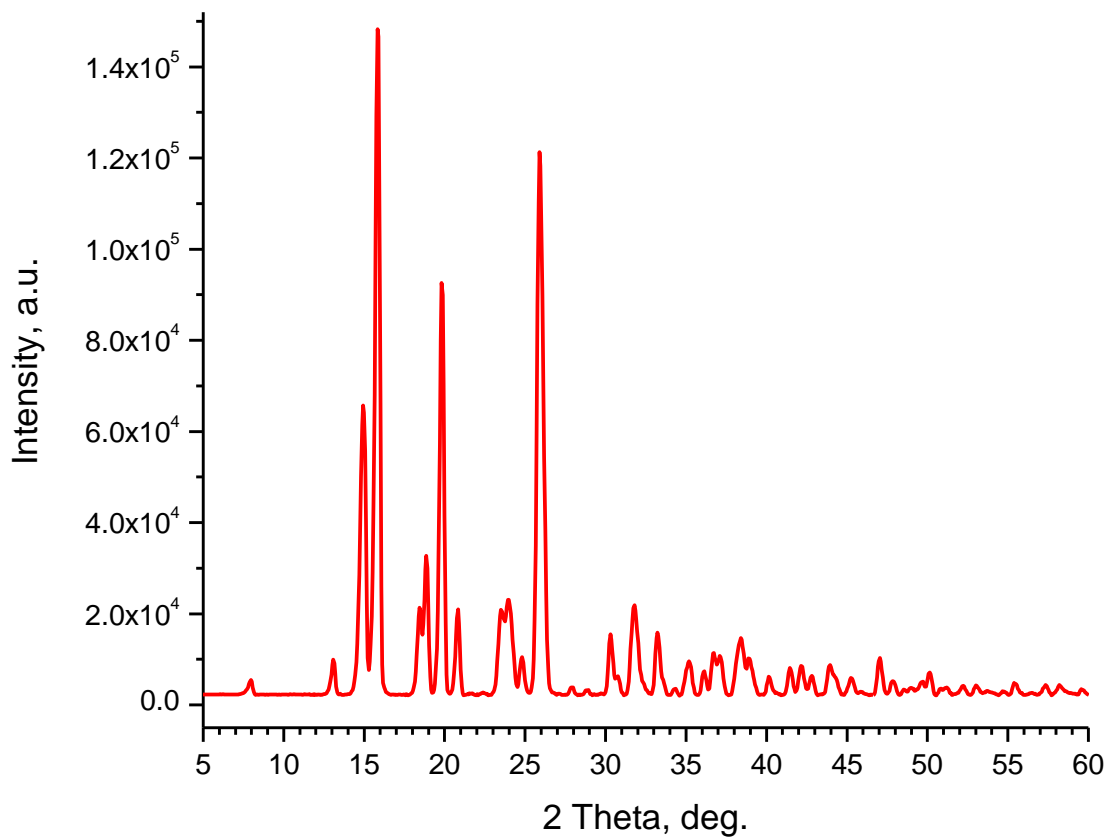


Figure S28. Experimental and calculated powder diffractograms of **6a**, $(\text{CuCN})_2(3\text{-EtPy})_3$.

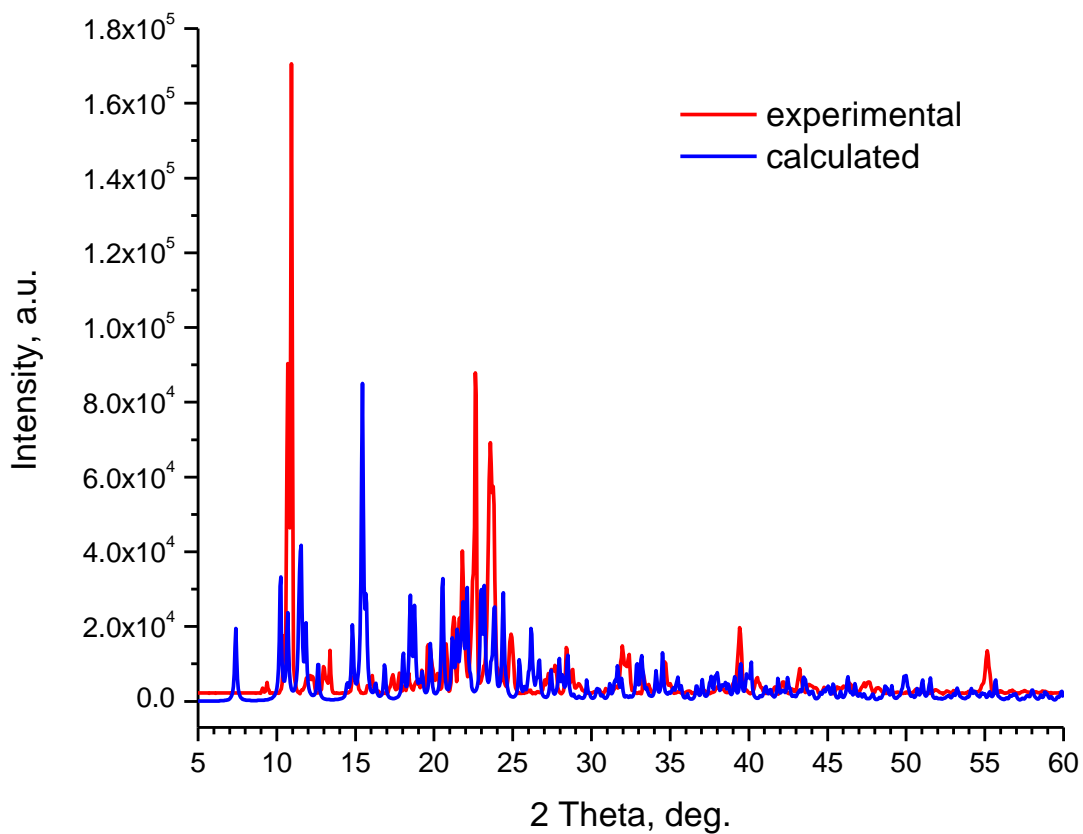


Figure S29. Powder diffractogram of **6b**, (CuCN)(3-EtPy).

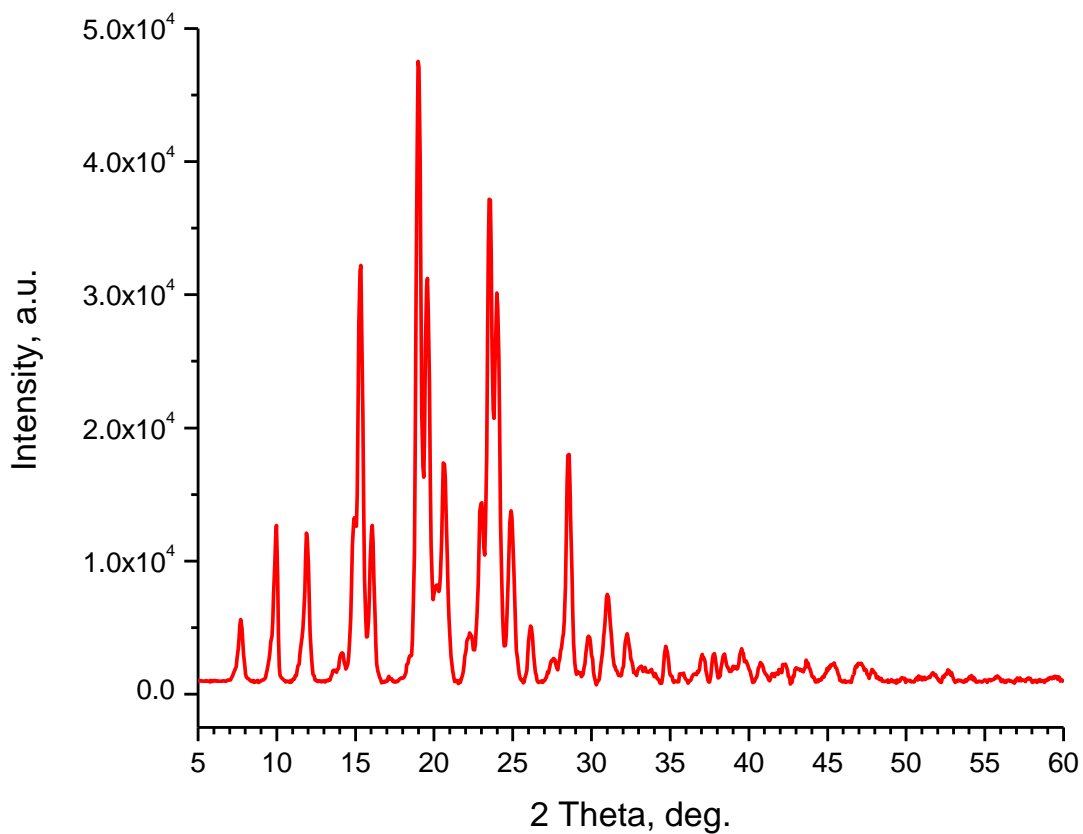


Figure S30. Powder diffractogram of **7**, (CuCN)(4-EtPy).

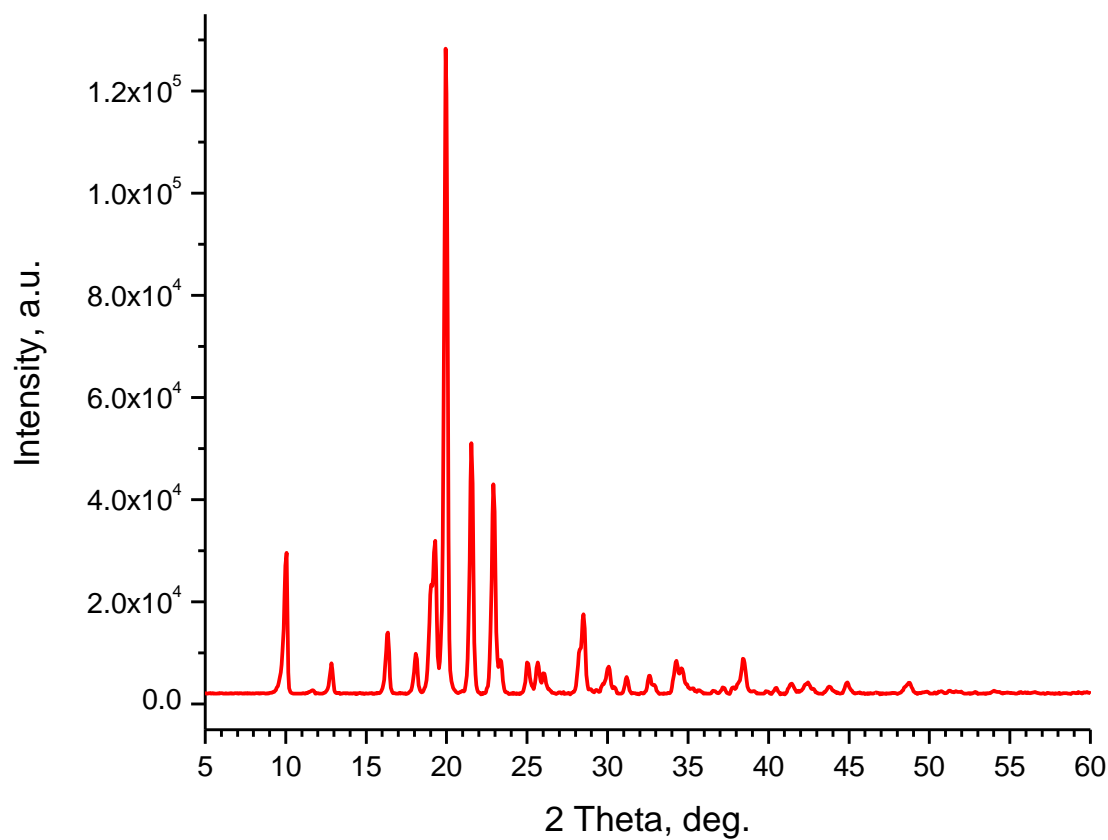


Figure S31. Experimental and calculated powder diffractograms of **8**, (CuCN)(4-*t*BuPy).

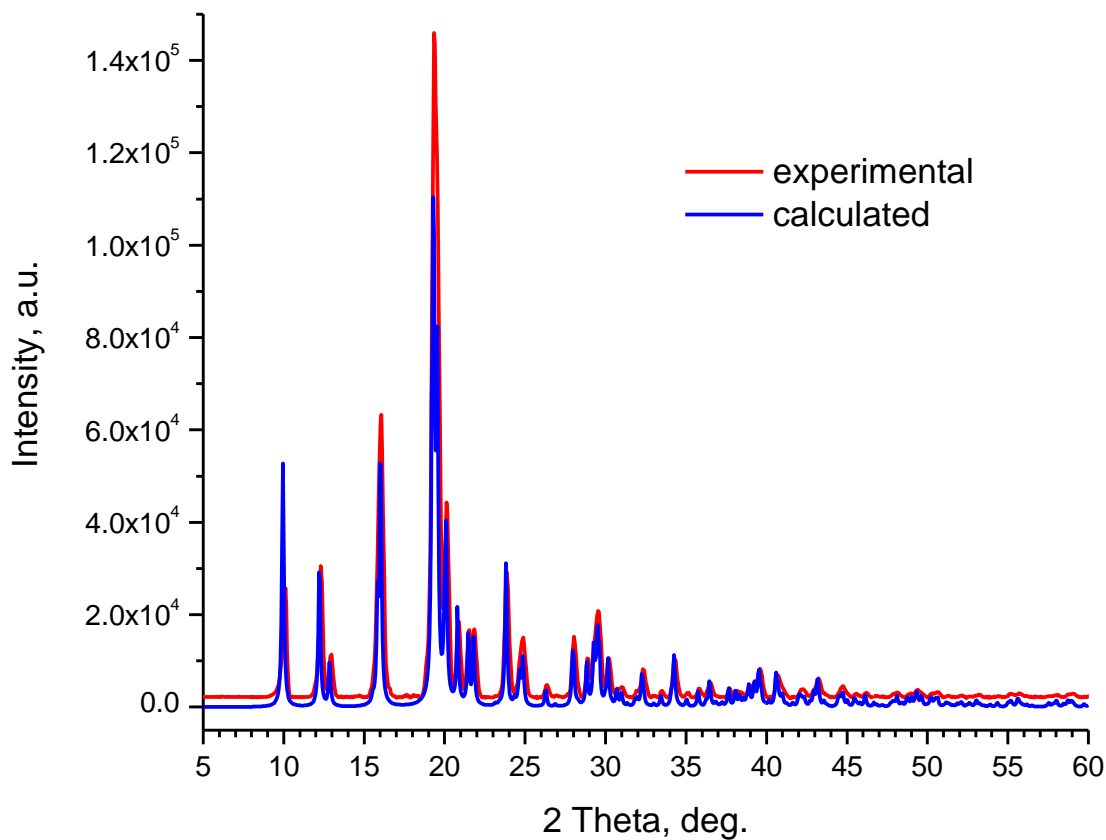


Figure S32. Experimental and calculated powder diffractograms of **9**, $(\text{CuCN})_3(\text{Pipd})_4$.

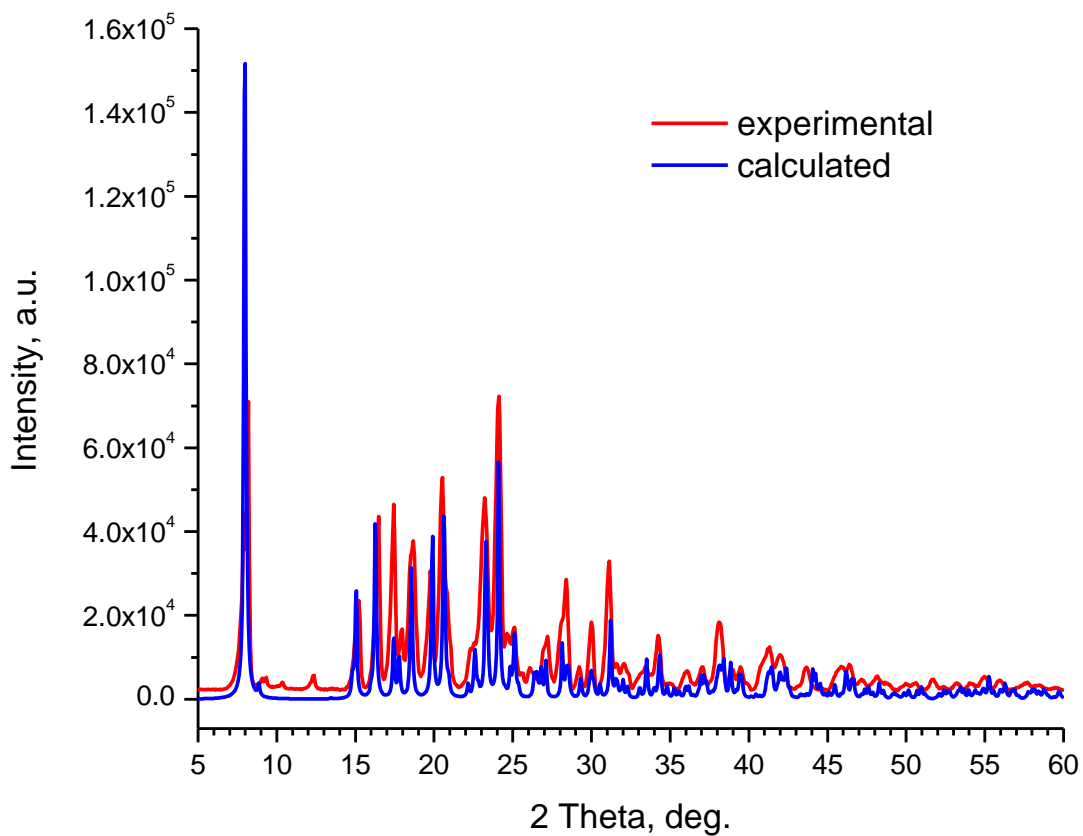


Figure S33. Powder diffractogram of **10**, (CuCN)(N-MePipd).

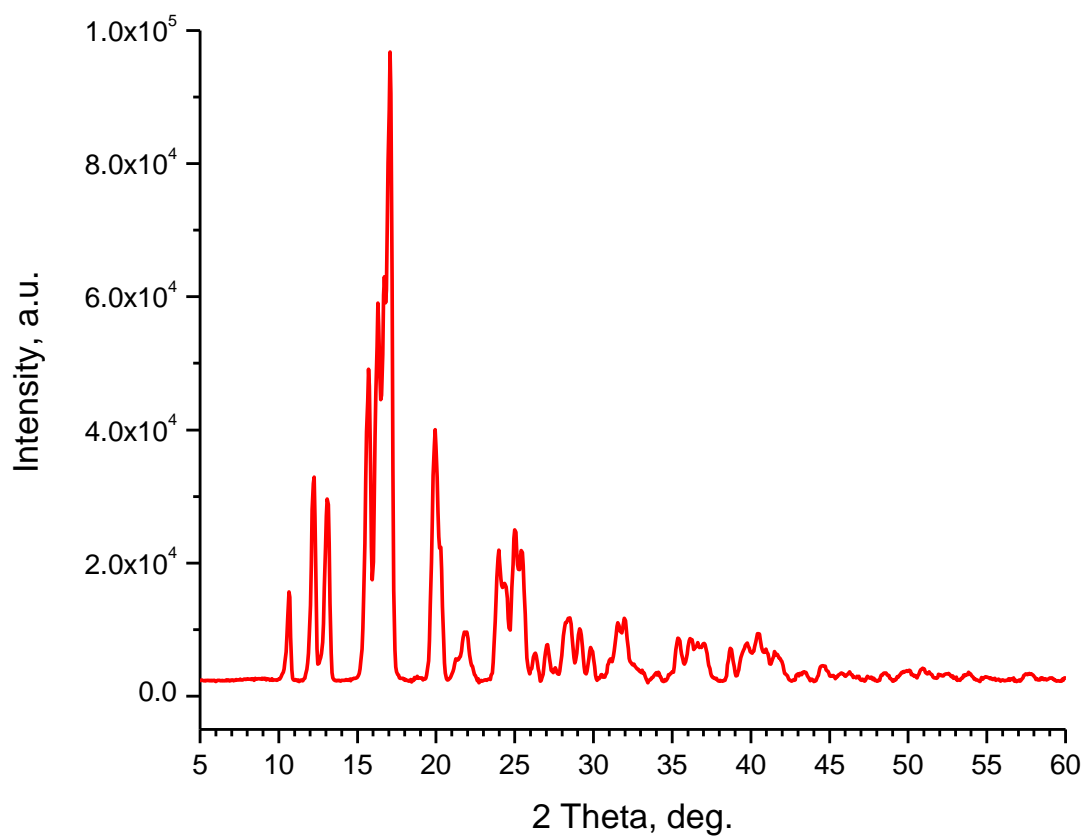


Figure S34. Powder diffractogram of **11**, $(\text{CuCN})_4(\text{N-EtPipd})_3$.

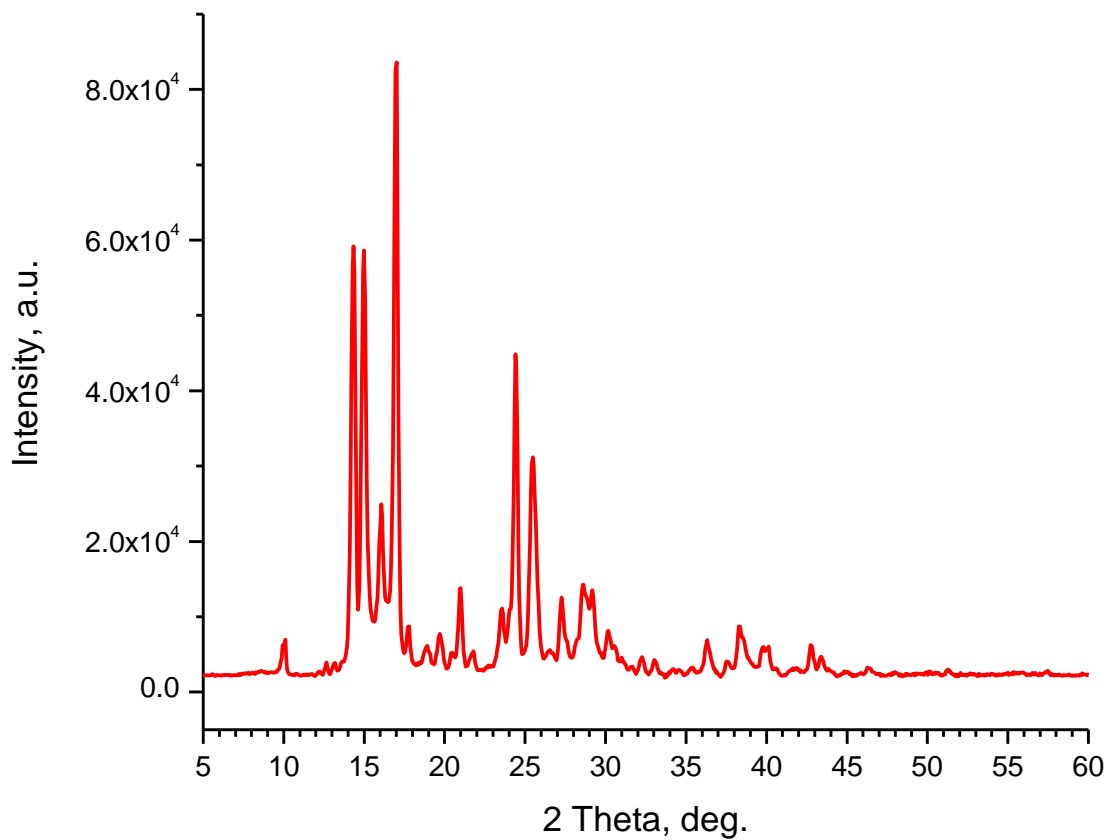


Figure S35. Experimental and calculated powder diffractograms of **12**, (CuCN)(MeMorph).

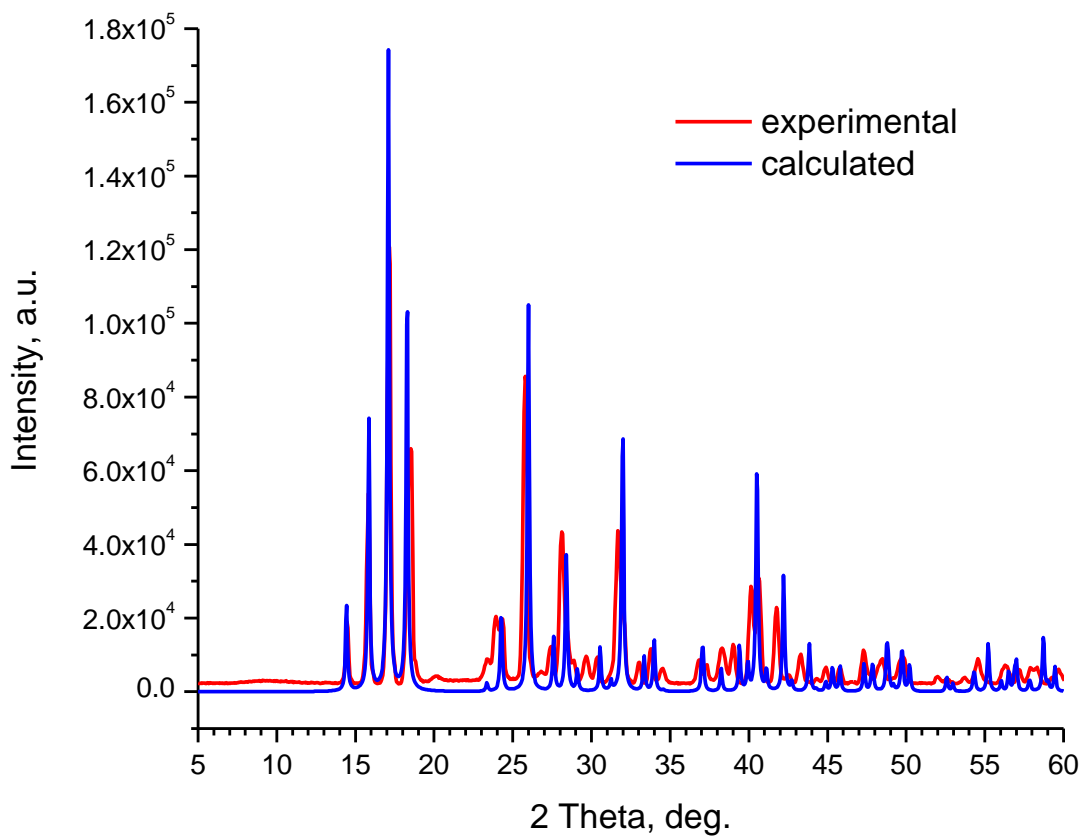


Figure S36. Experimental and calculated powder diffractograms of **13**, (CuCN)(Me₂NCy).

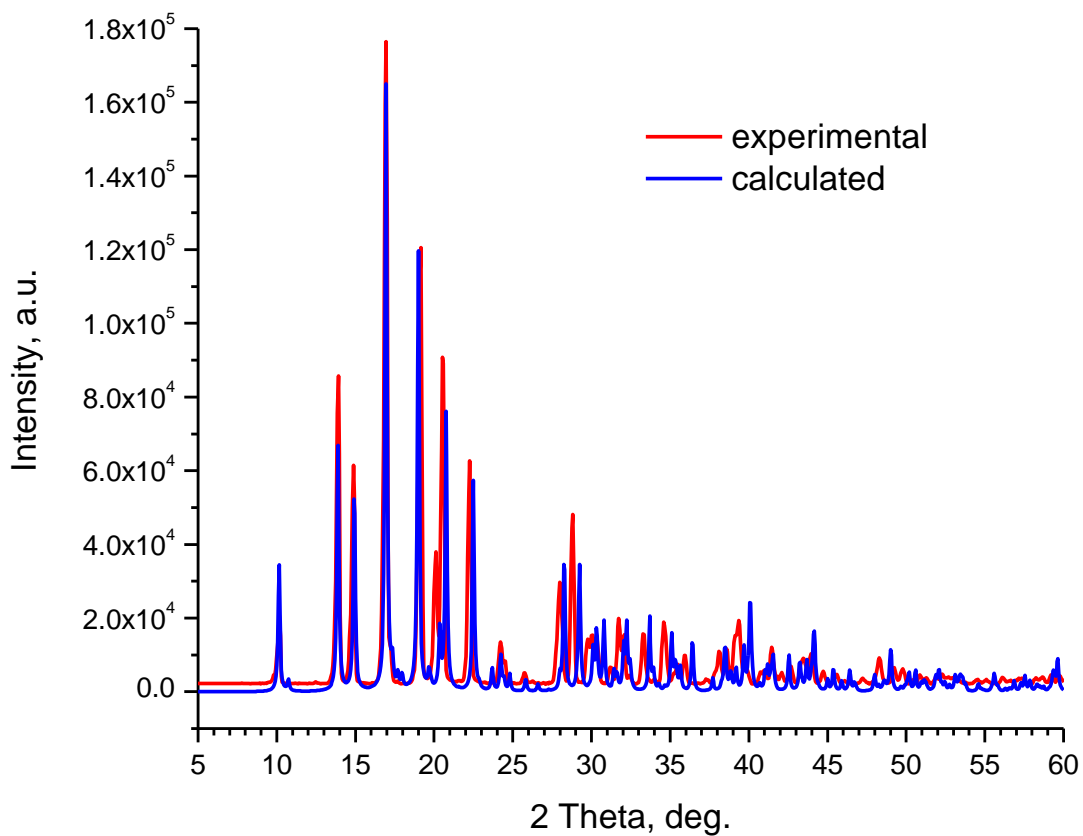


Figure S37. PXRD traces for CuCN and Py. Key: black = CuCN only, red = authentic **1b**, blue = CuCN powder + liquid Py, green = CuCN pellet + Py vapor.

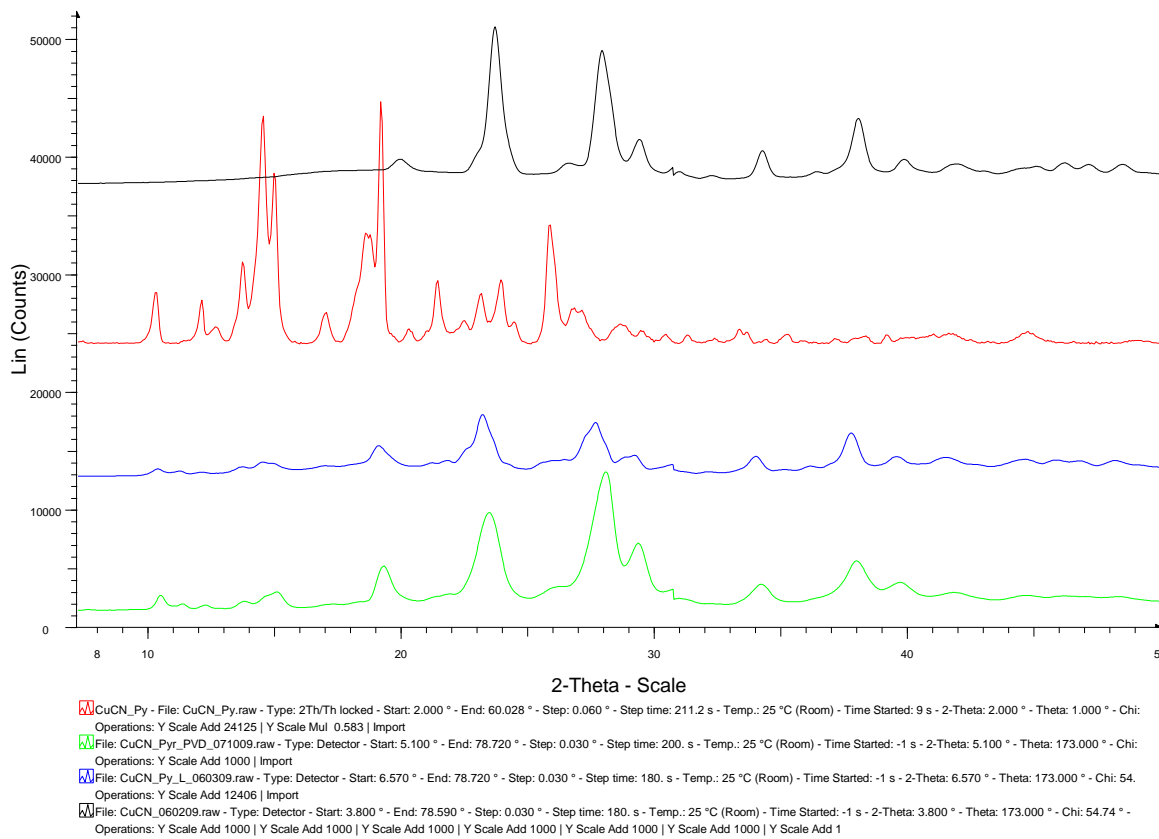


Figure S38. PXRD traces for CuCN and 2-MePy. Key: black = CuCN only, red = authentic **2b**, blue = CuCN powder + liquid 2-MePy, green = CuCN pellet + 2-MePy vapor.

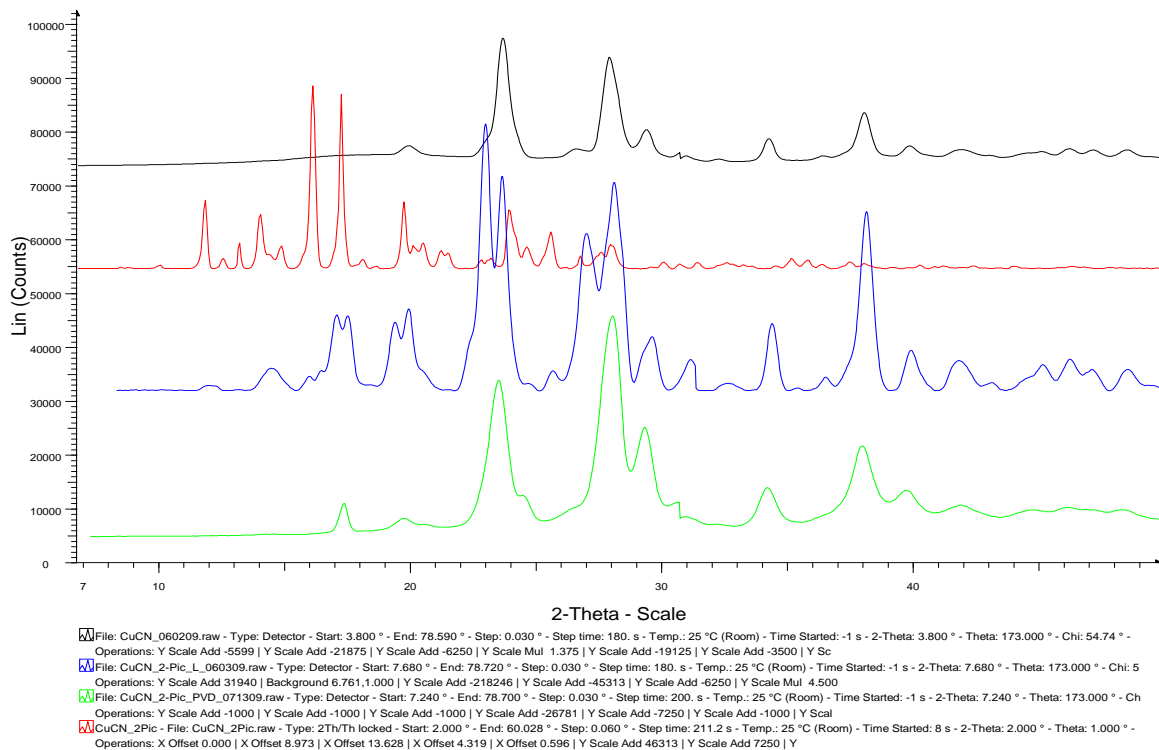


Figure S39. PXRD traces for CuCN and 3-MePy. Key: black = CuCN only, red = authentic **3a**, blue = CuCN powder + liquid 3-MePy, green = CuCN pellet + 3-MePy vapor.

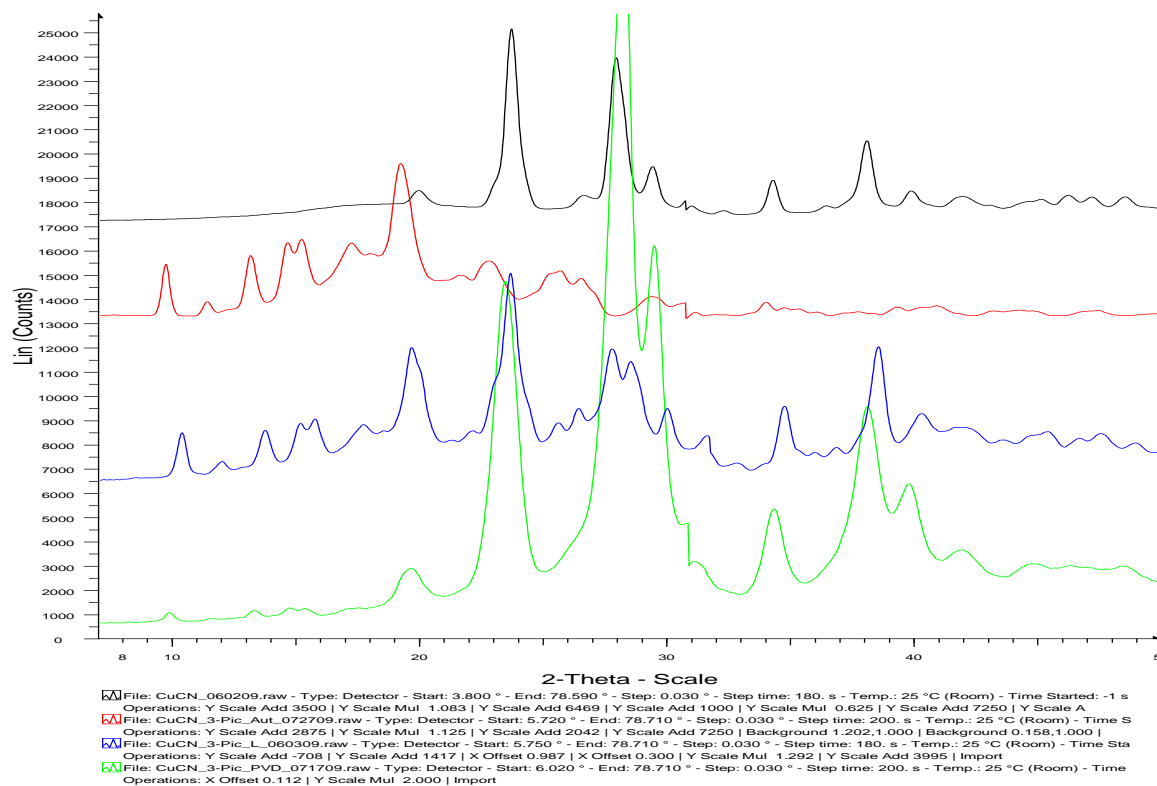


Figure S40. PXRD traces for CuCN and 2-EtPy. Key: black = CuCN only, red = authentic **5**, blue = CuCN powder + liquid 2-EtPy, green = CuCN pellet + 2-EtPy vapor.

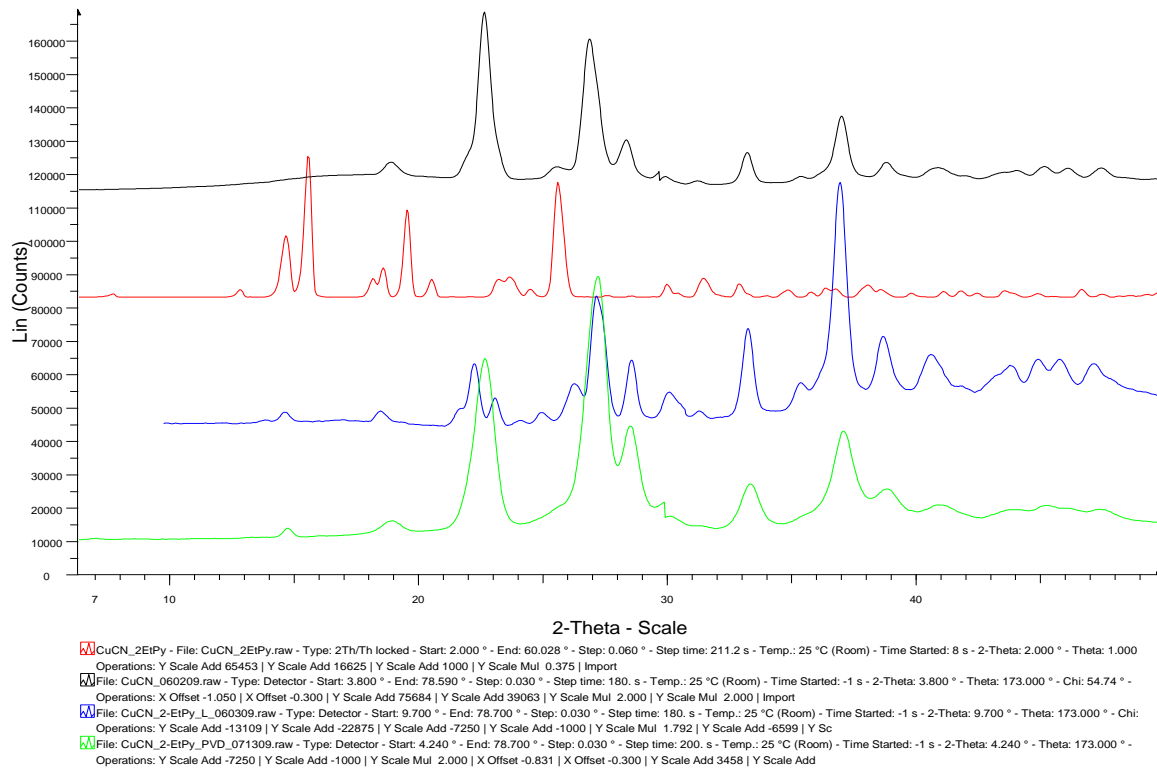


Figure S41. PXRD traces for CuCN and 4-EtPy. Key: black = CuCN only, red = authentic **7**, blue = CuCN powder + liquid 4-EtPy, green = CuCN pellet + 4-EtPy vapor.

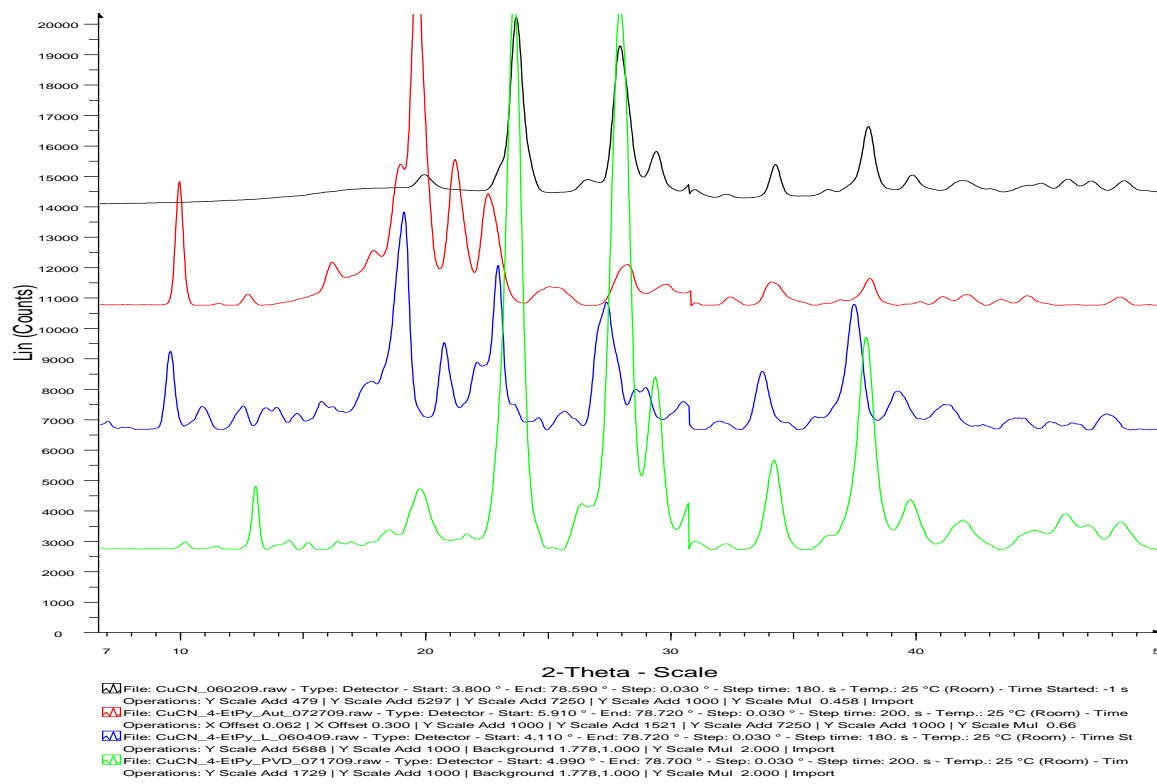


Figure S42. PXRD traces for CuCN and 4-^tBuPy. Key: black = CuCN only, red = authentic **8**, blue = CuCN powder + liquid 4-^tBuPy, green = CuCN pellet + 4-^tBuPy vapor.

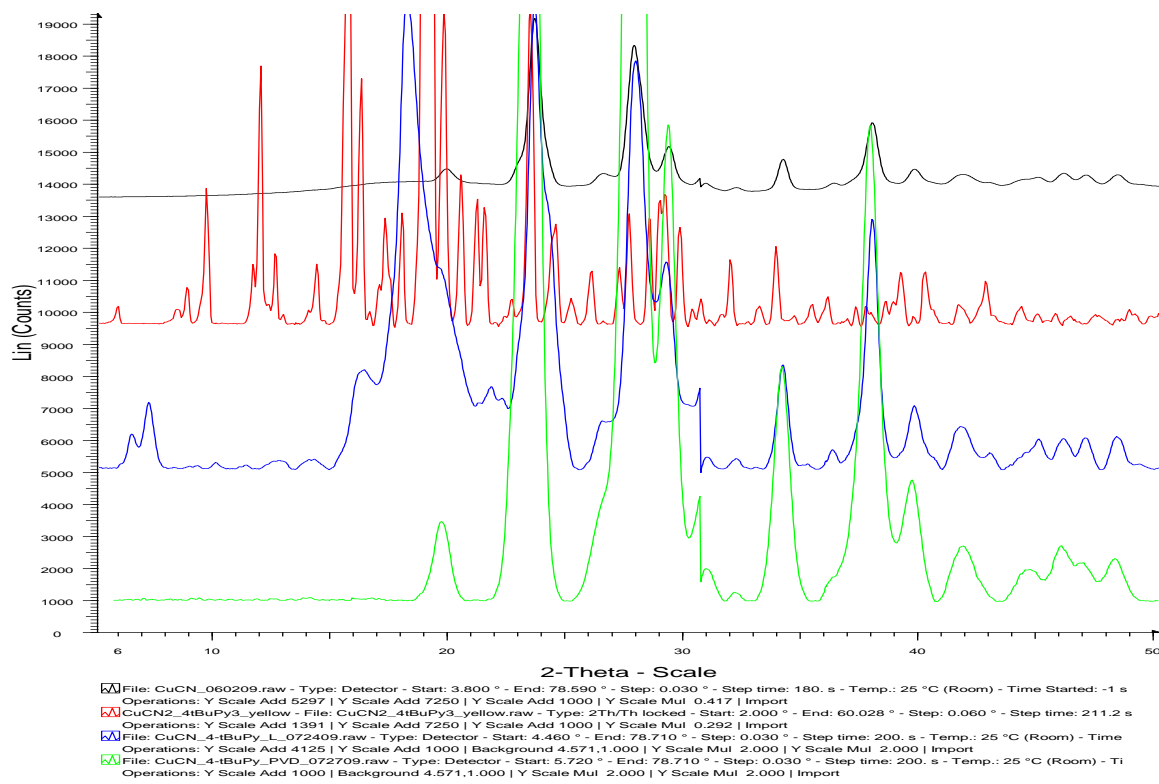


Figure S43. PXRD traces for CuCN and Pipd. Key: black = CuCN only, red = authentic **9**, blue = CuCN powder + liquid Pipd, green = CuCN pellet + Pipd vapor.

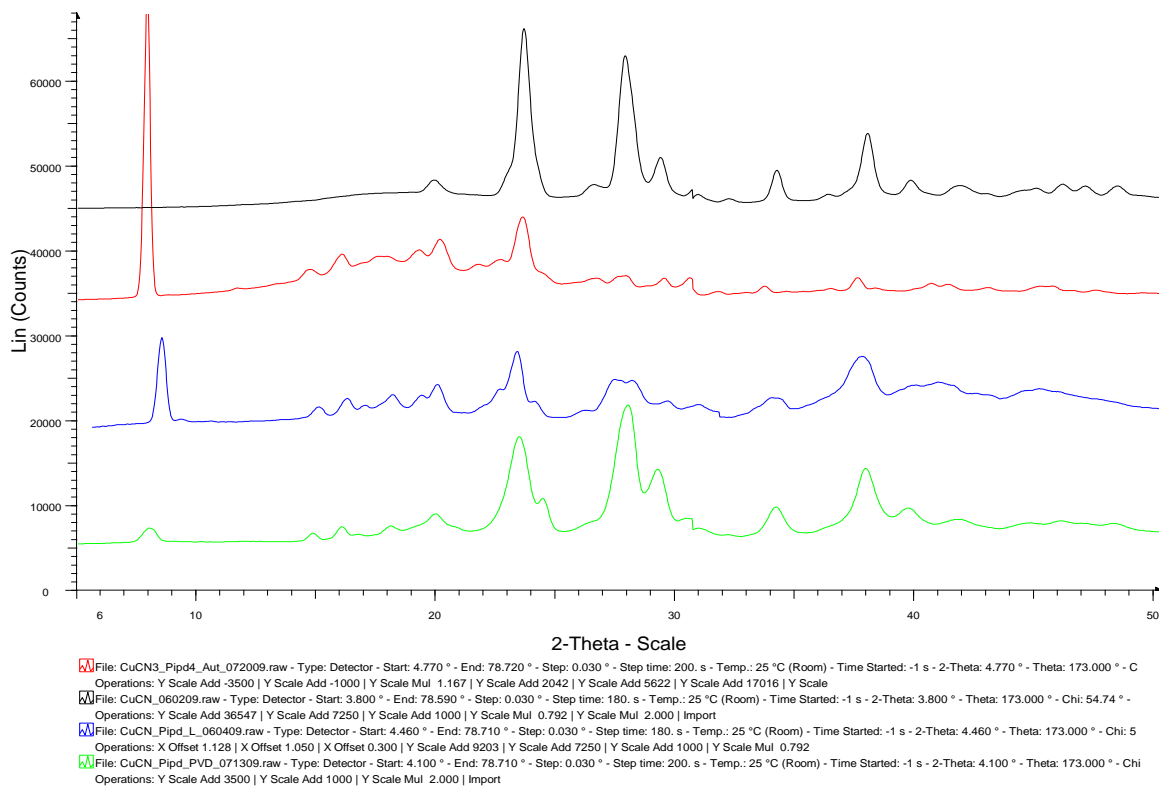


Figure S44. PXRD traces for CuCN and N-MePipd. Key: black = CuCN only, red = authentic **10**, blue = CuCN powder + liquid N-MePipd, green = CuCN pellet + N-MePipd vapor.

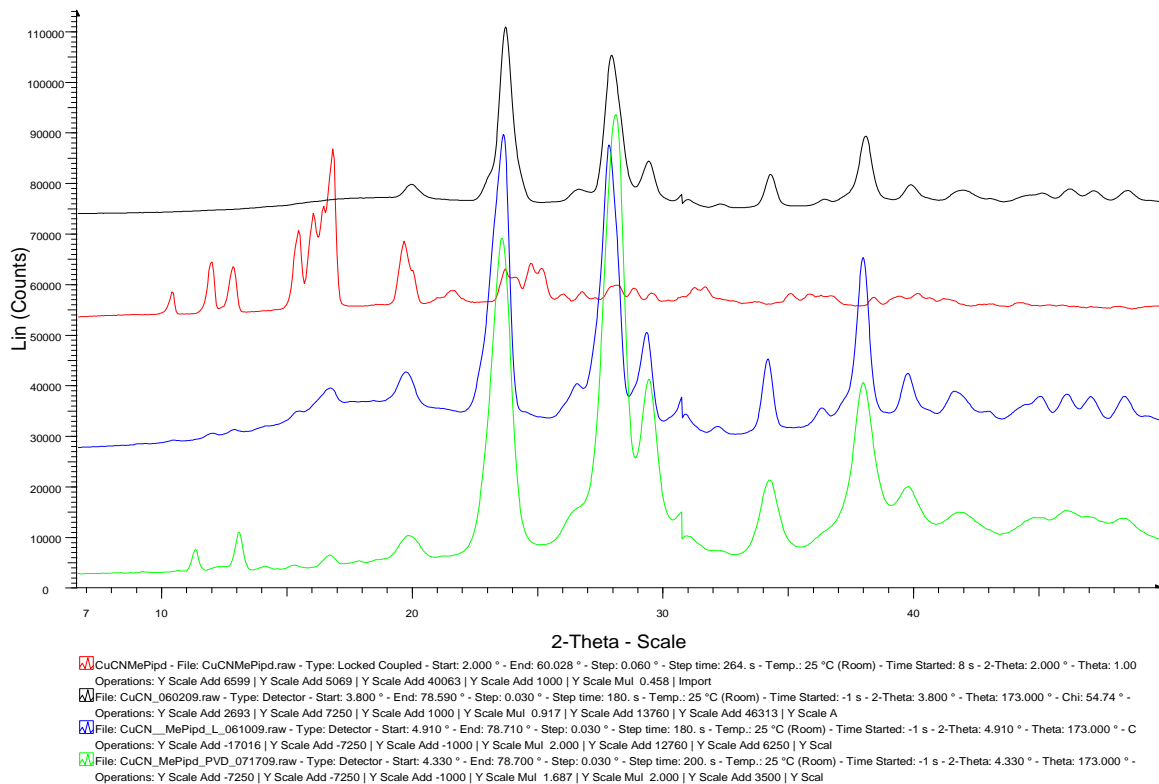


Figure S45. PXRD traces for CuCN and N-EtPipd. Key: black = CuCN only, red = authentic **11**, blue = CuCN powder + liquid N-EtPipd, green = CuCN pellet + N-EtPipd vapor.

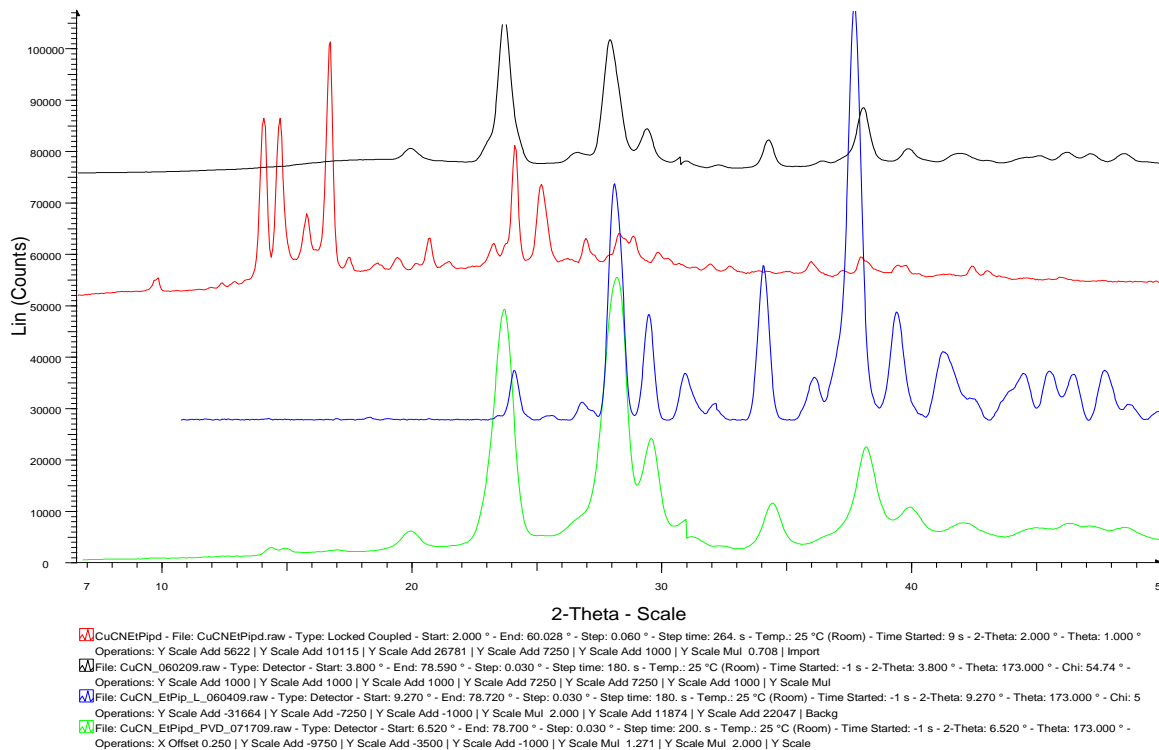


Figure S46. PXRD traces for CuCN and MeMorph. Key: black = CuCN only, red = authentic **12**, blue = CuCN powder + liquid MeMorph, green = CuCN pellet + MeMorph vapor.

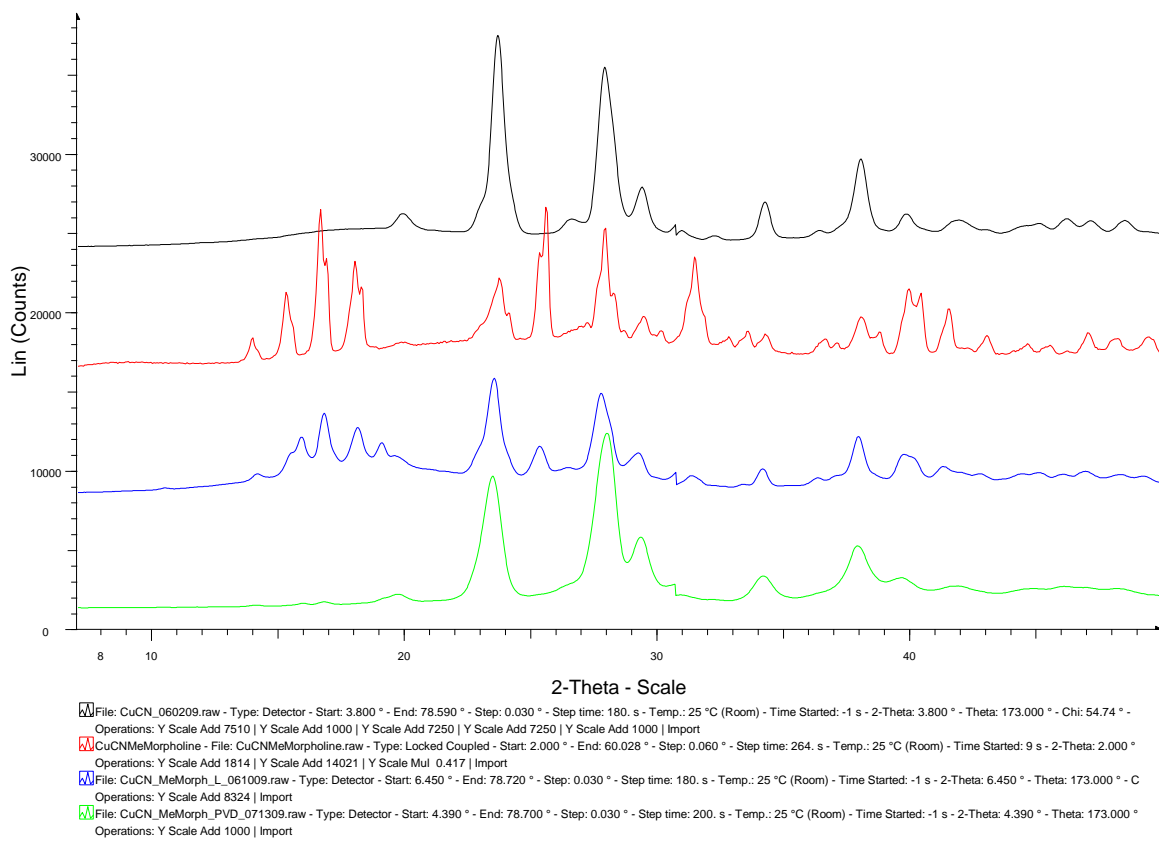


Figure S47. PXRD traces for CuCN and Me₂NCy. Key: black = CuCN only, red = authentic **13**, blue = CuCN powder + liquid Me₂NCy, green = CuCN pellet + Me₂NCy vapor.

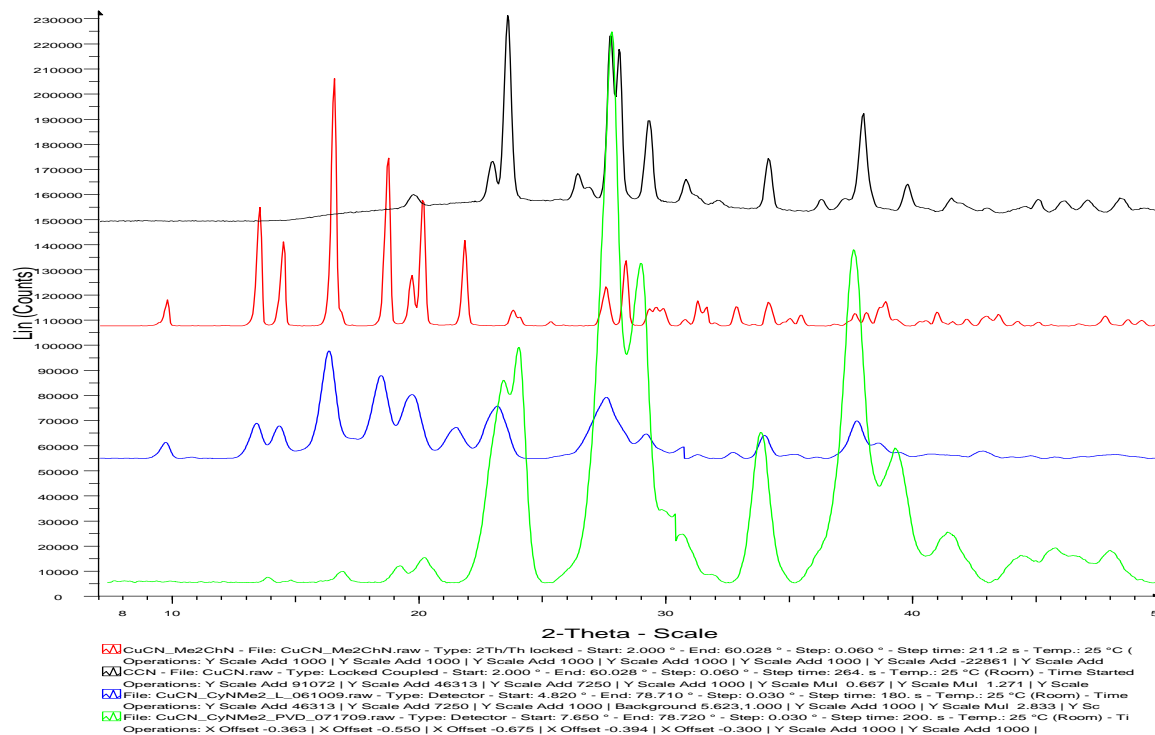


Figure S48. Luminescence Spectra of **1b** ($\text{CuCN}(\text{Py})_5$) at 298 K and 77K.

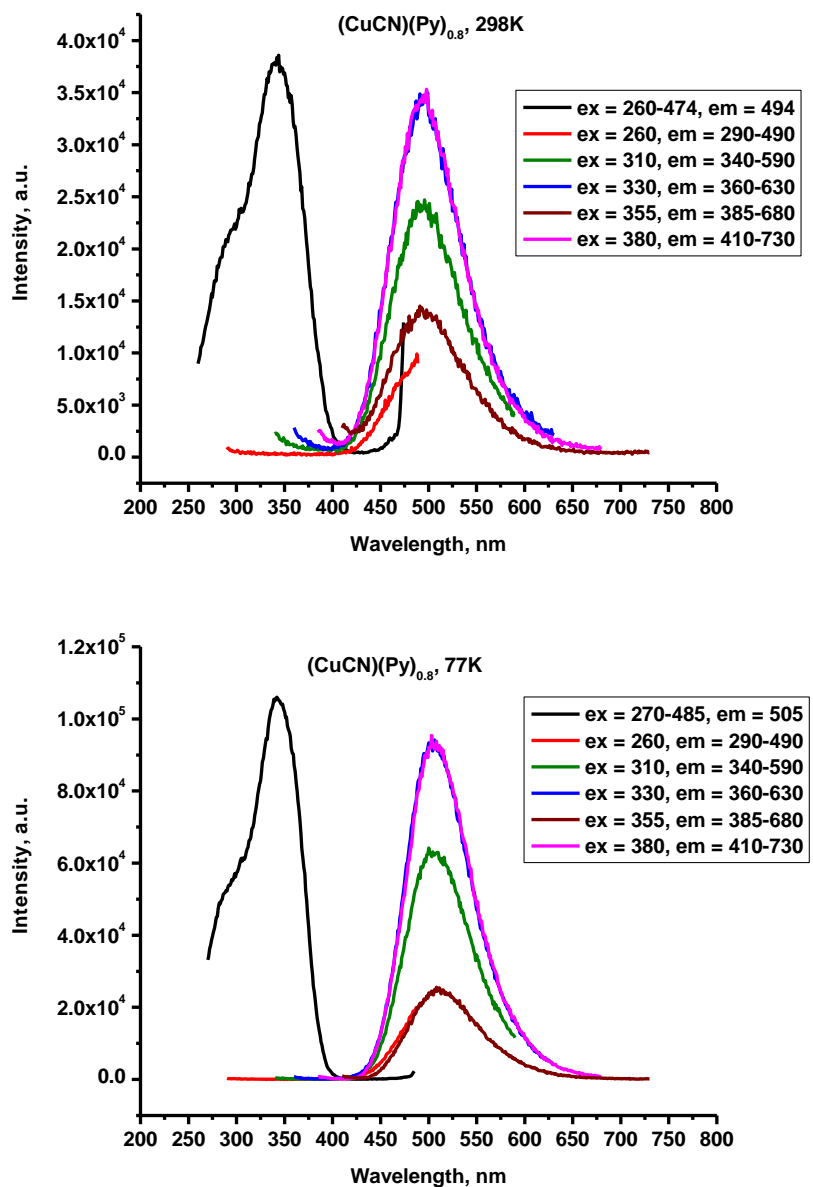


Figure S49. Luminescence Spectra of **2a** ($\text{CuCN}_2(2\text{-MePy})_3$) at 298 K and 77K.

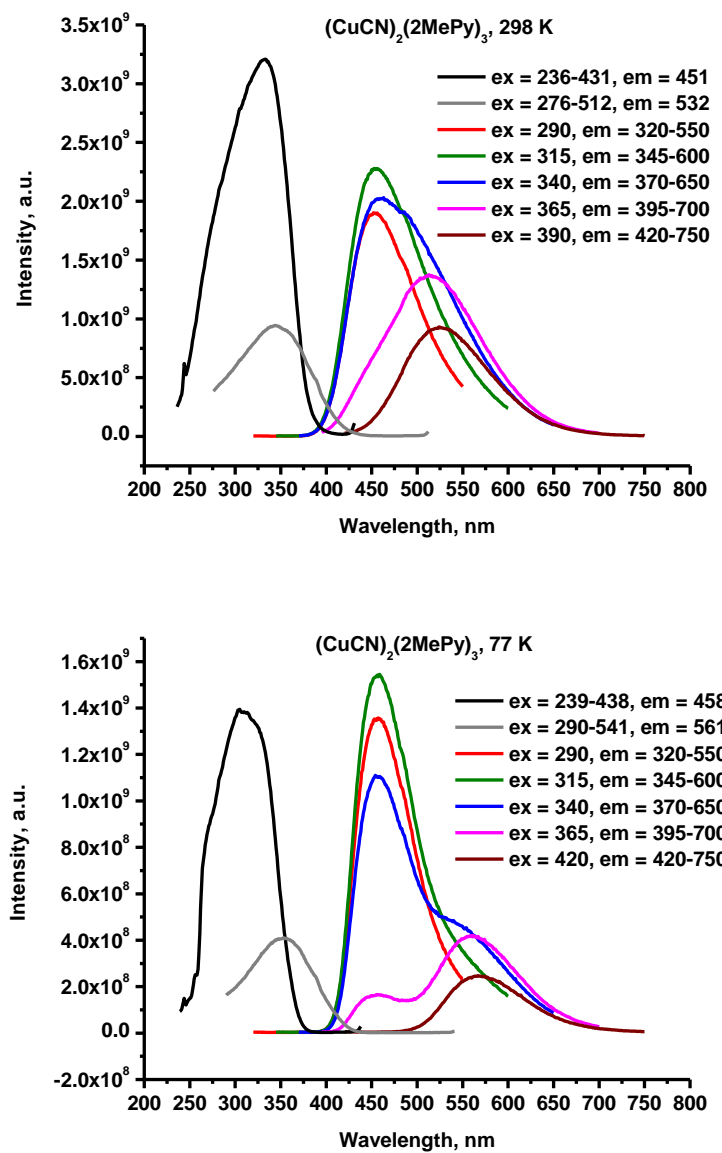


Figure S50. Luminescence Spectra of **2b** ($\text{CuCN}(2\text{-MePy})$) at 298 K and 77K.

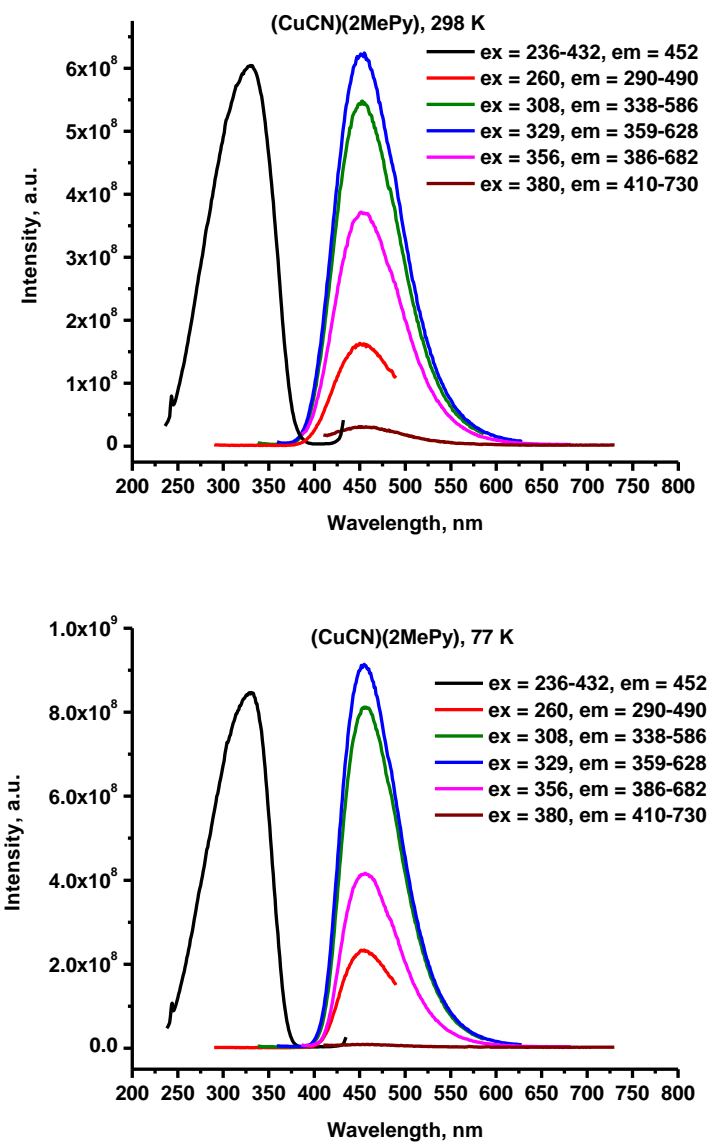


Figure S51. Luminescence Spectra of **3a** ($\text{CuCN}_2(3\text{-MePy})_3$) at 298 K and 77K.

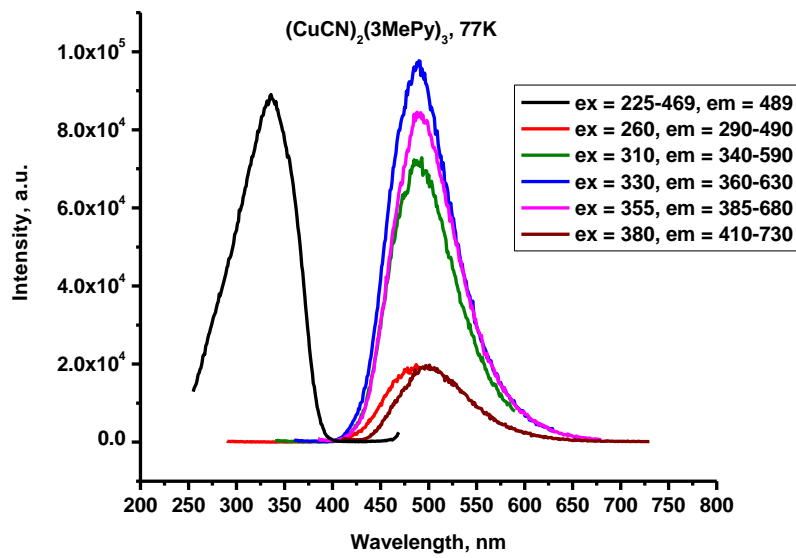
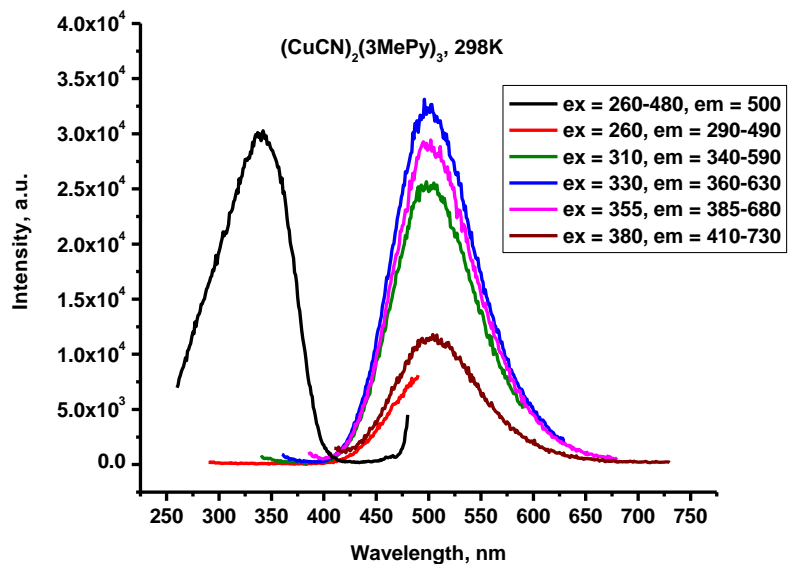


Figure S52. Luminescence Spectra of **4** (CuCN)₂(4-MePy)₃ at 77K. (Compound **4** exhibits no luminescence at 298 K.)

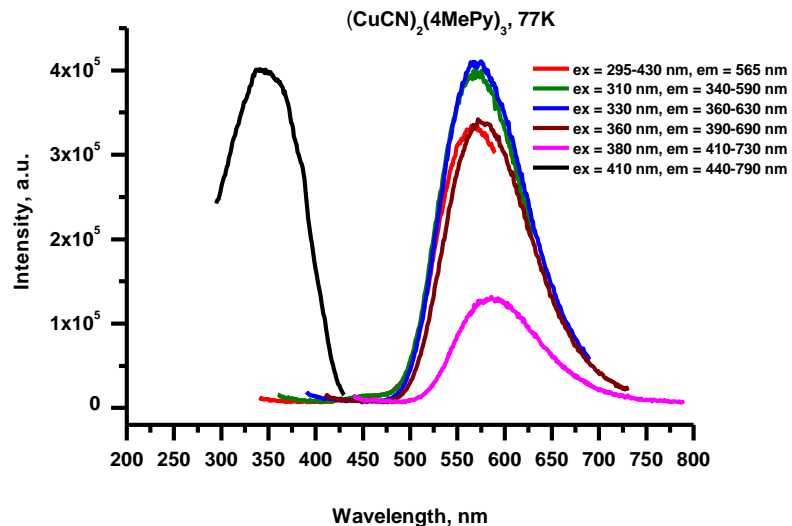


Figure S53. Luminescence Spectra of **5** ($\text{CuCN}(\text{2-EtPy})_3$) at 298 K and 77K.

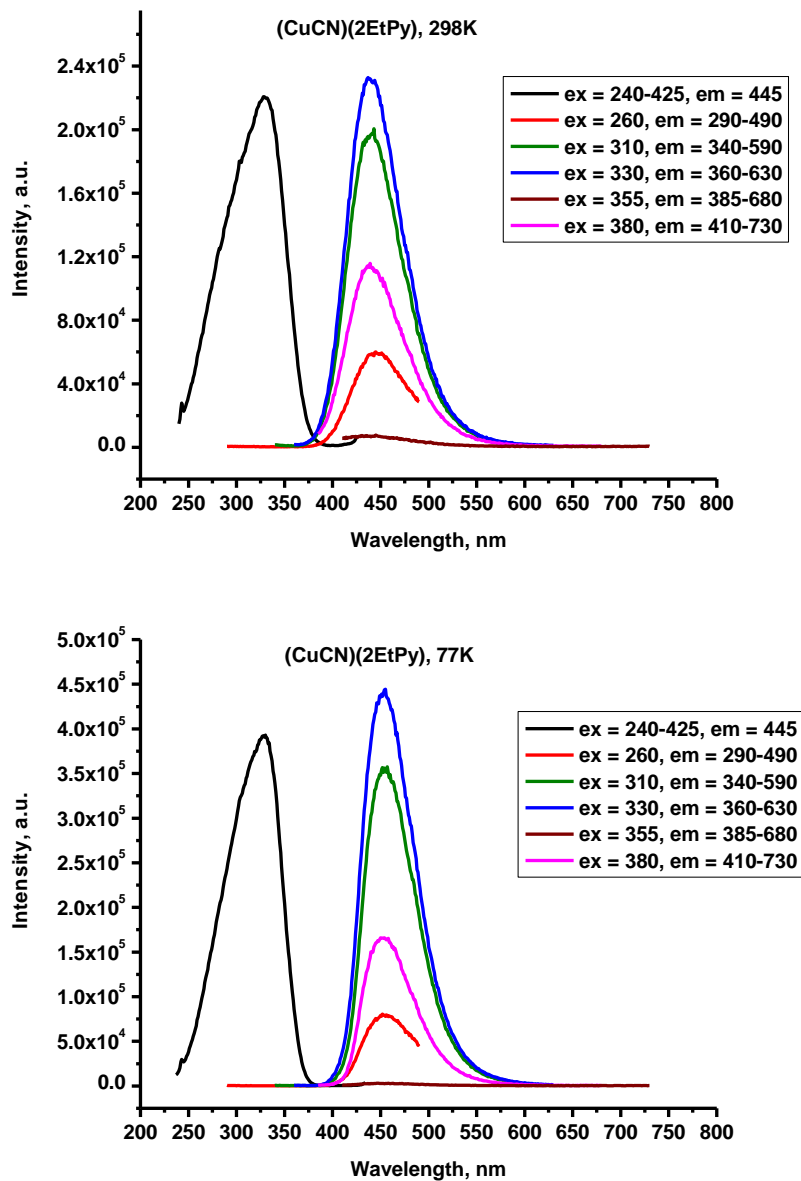


Figure S54. Luminescence Spectra of **6b** ($\text{CuCN}(3\text{-EtPy})$) at 298 K and 77K.

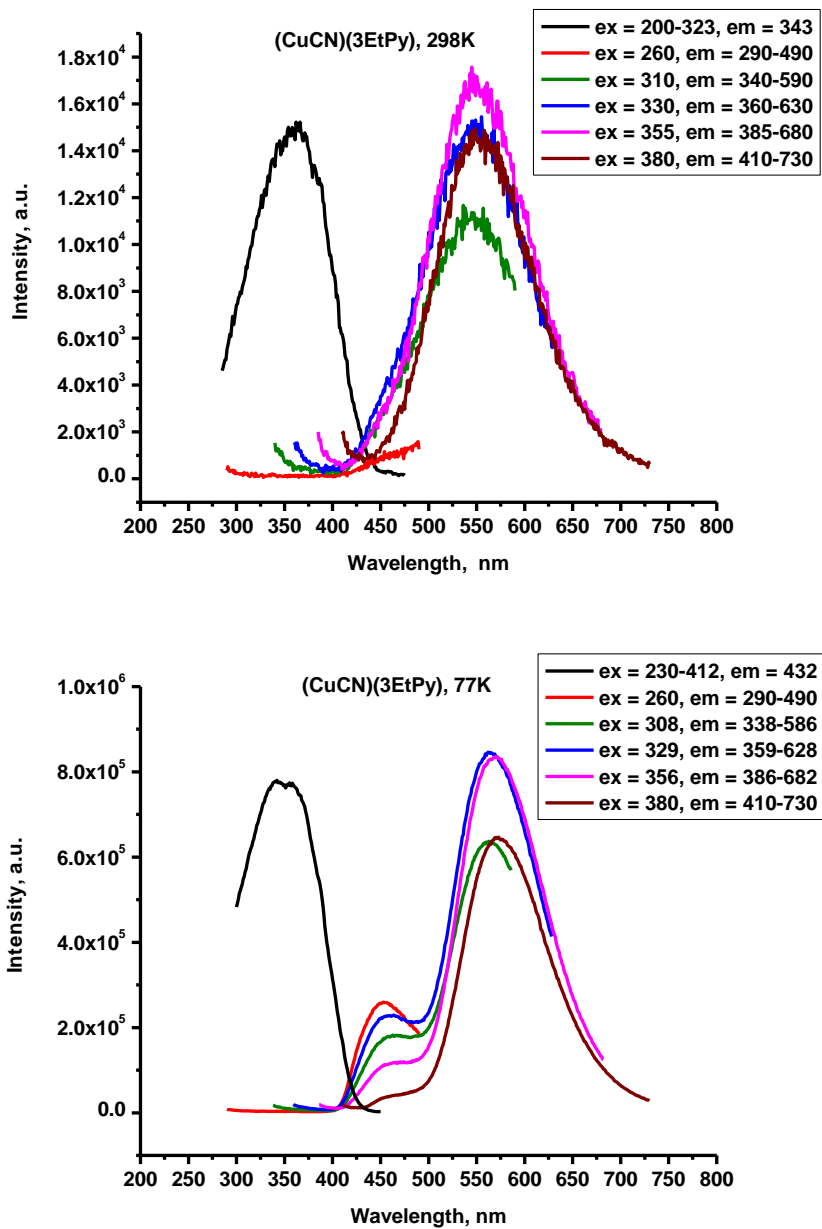


Figure S55. Luminescence Spectra of **9** (CuCN)₂(4-*t*BuPy)₃ at 298 K and 77K.

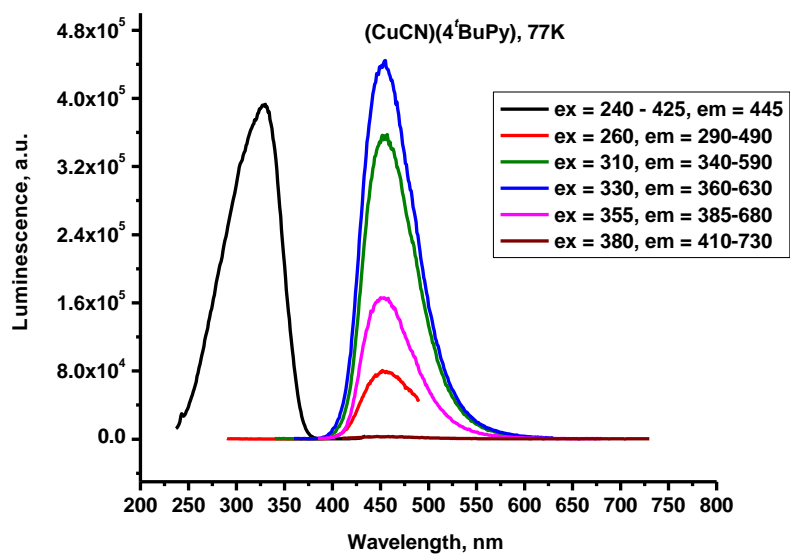
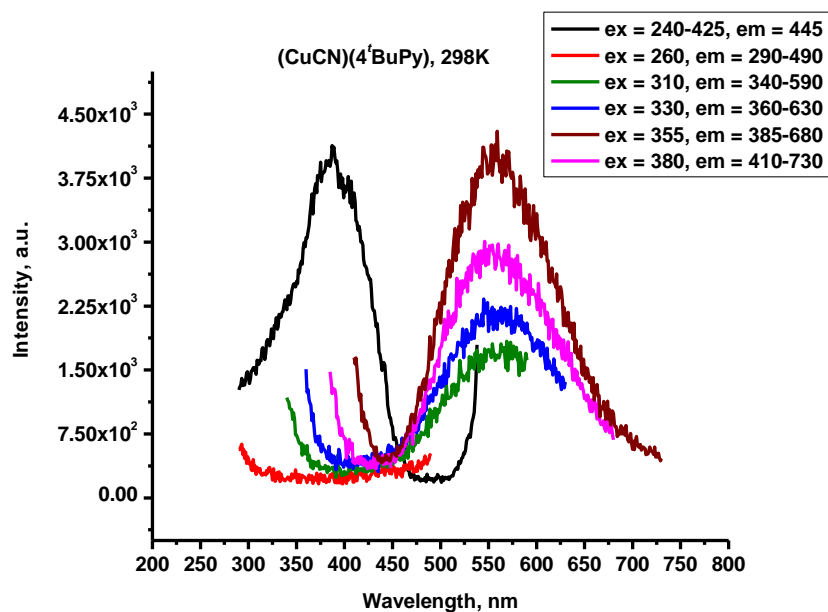


Figure S56. Luminescence Spectra of **16** ($\text{CuCN}_3(\text{Pipd})_4$) at 298 K and 77K.

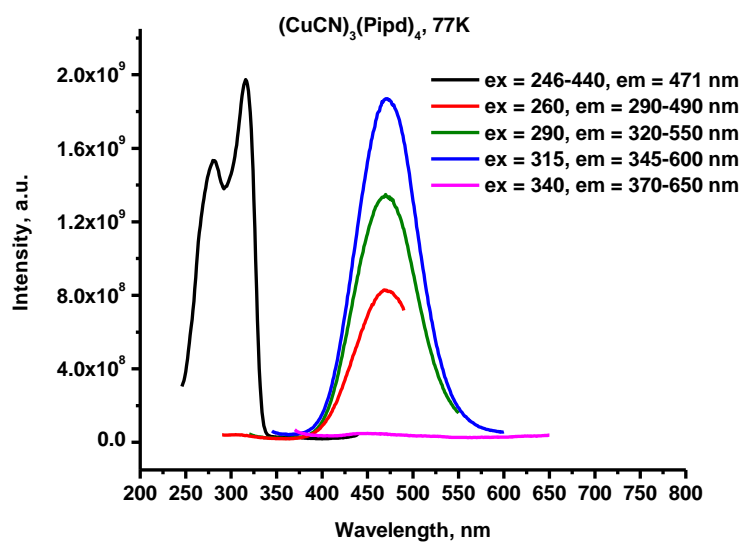
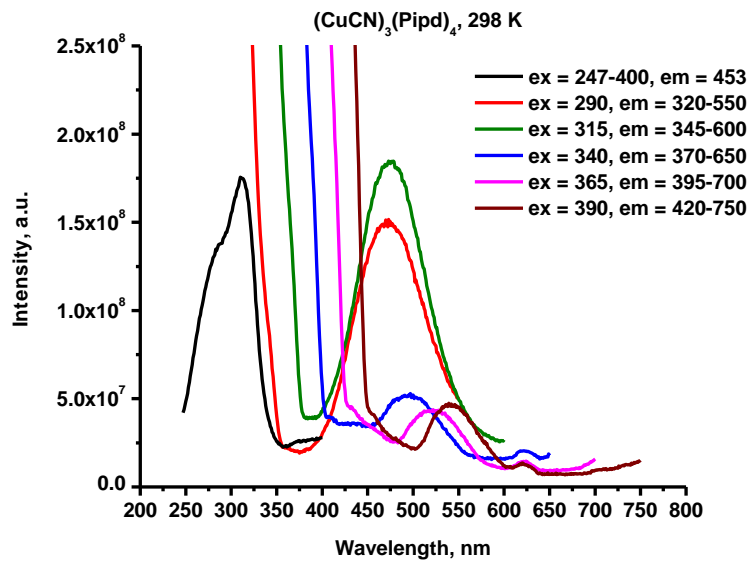


Figure S57. Luminescence Spectra of **17** ($\text{CuCN}(\text{N-MePipd})$) at 298 K and 77K.

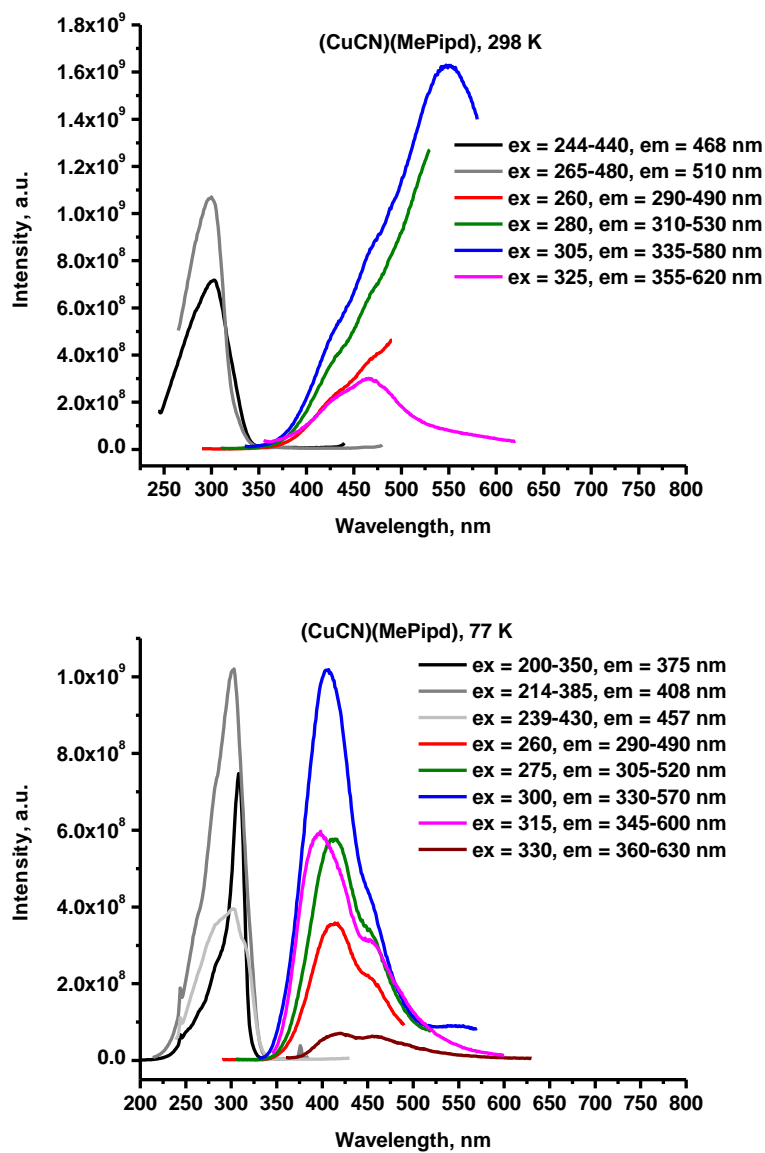


Figure S58. Luminescence Spectra of **18** ($\text{CuCN}_4(\text{EtPipd})_3$) at 298 K and 77K.

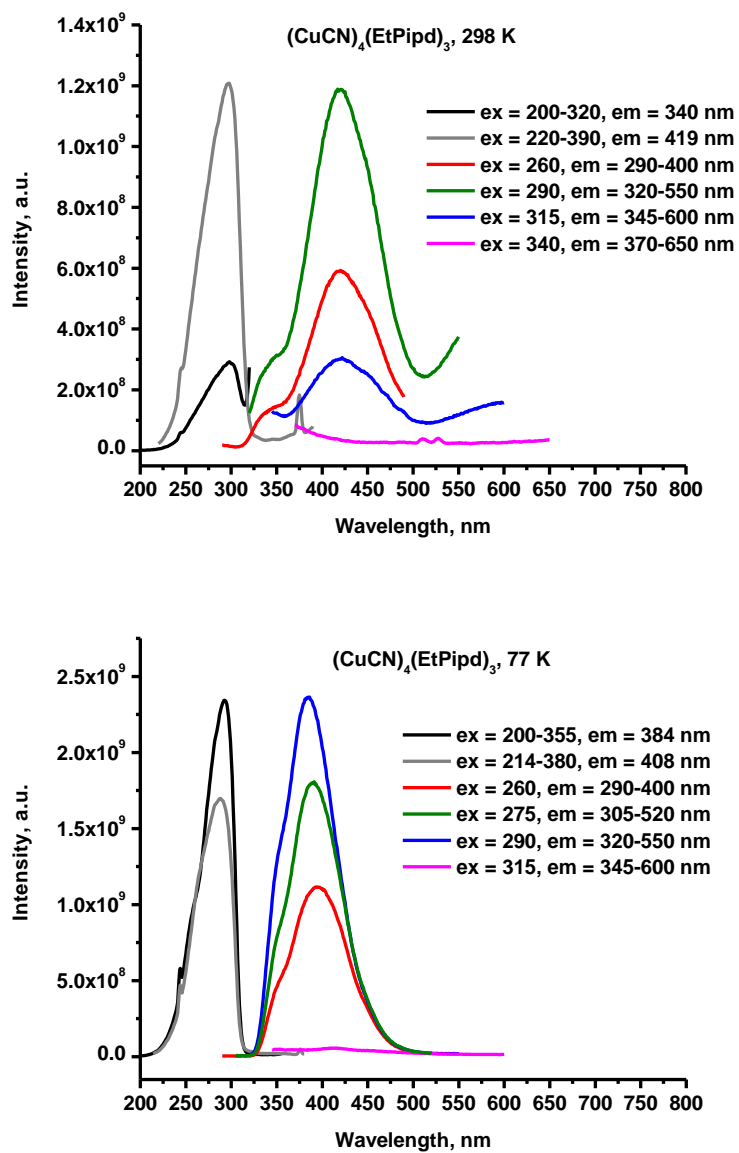


Figure S59. Luminescence Spectra of **21** ($\text{CuCN}(\text{MeMorph})$) at 298 K and 77K.

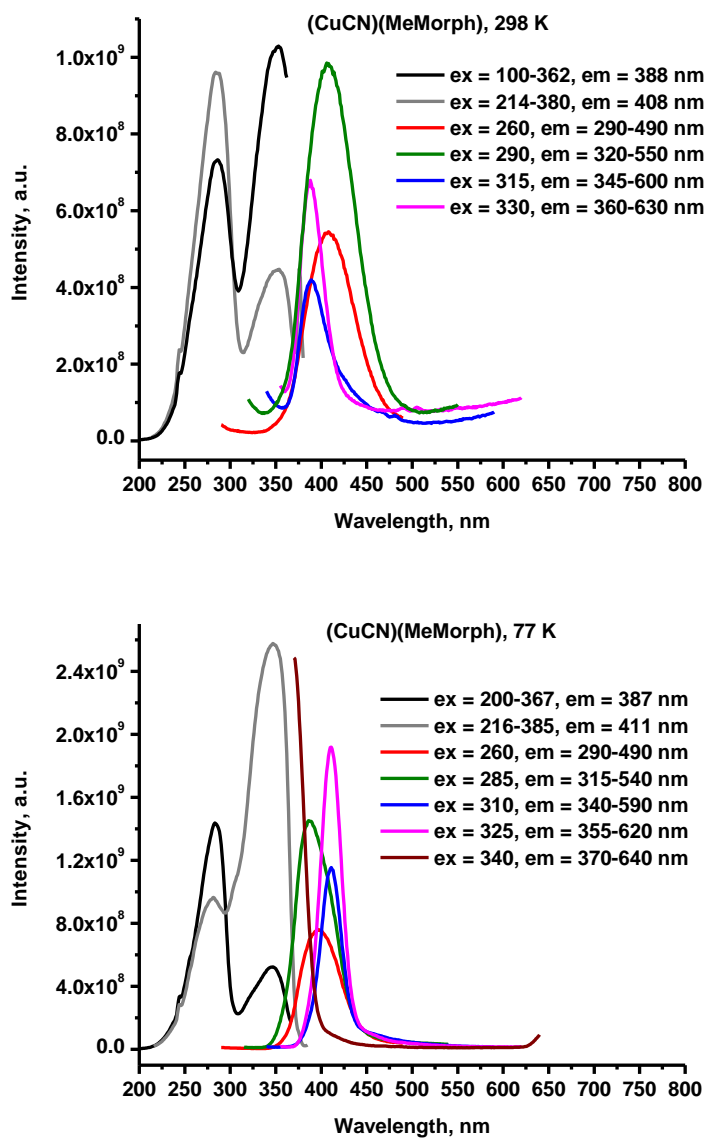


Figure S60. Luminescence Spectra of **22** ($\text{CuCN}(\text{Me}_2\text{NCy})$) at 298 K and 77K.

